AFWAL-TR-80-4053

DYNAMIC TENSILE TESTING OF STRUCTURAL MATERIALS USING A SPLIT HOPKINSON BAR APPARATUS

T. Nicholas

Metals Behavior Branch
Metals and Ceramics Division

October 1980

TECHNICAL REPORT AFWAL-TR-80-4053

Interim Report for Period January 1973 - December 1979

Approved for public release; distribution unlimited.

MATERIALS LABORATORY
AIR FORCE WRIGHT AERONAUTICAL LABORATORIES
AIR FORCE SYSTEMS COMMAND
WRIGHT-PATTERSON AIR FORCE BASE, OHIO 45433

NOTICE

When Government drawings, specifications, or other data are used for any purpose other than in connection with a definitely related Government procurement operation, the United States Government thereby incurs no responsibility nor any obligation whatsoever; and the fact that the government may have formulated, furnished, or in any way supplied the said drawings, specifications, or other data, is not to be regarded by implication or otherwise as in any manner licensing the holder or any other person or corporation, or conveying any rights or permission to manufacture use, or sell any patented invention that may in any way be related thereto.

This report has been reviewed by the Office of Public Affairs (ASD/PA) and is releasable to the National Technical Information Service (NTIS). At NTIS, it will be available to the general public, including foreign nations.

This technical report has been reviewed and is approved for publication.

JOHN P. HENDERSON, Acting Chief
Metals Behavior Branch
Metals and Ceramics Division

THEODORE NICHOLAS, Project Engineer
Metals Behavior Branch
Metals and Ceramics Division

"If your address has changed, if you wish to be removed from our mailing list, or if the addressee is no longer employed by your organization please notify AFWAL/MLLN, W-PAFB, OH 45433 to help us maintain a current mailing list".

Copies of this report should not be returned unless return is required by security considerations, contractual obligations, or notice on a specific document.

AIR FORCE/56780/20 November 1980 — 400

SECURITY CLASSIFICATION OF THIS PAGE (When Data Entered)

REPORT DOCUMENTATION PAGE

READ INSTRUCTIONS BEFORE COMPLETING FORM

1. REPORT NUMBER: AFWAL-TR-80-4053	2. GOVT ACCESSION NO.: AD-A092 832
3. RECIPIENT'S CATALOG NUMBER:	
4. TITLE (and Subtitle): DYNAMIC TENSILE TESTING OF STRUCTURAL MATERIALS USING A SPLIT HOPKINSON BAR APPARATUS	5. TYPE OF REPORT & PERIOD COVERED: Interim Report for period Jan 73-Dec 79
	6. PERFORMING ORG. REPORT NUMBER:
7. AUTHOR(s): Theodore Nicholas	8. CONTRACT OR GRANT NUMBER(s): P1
9. PERFORMING ORGANIZATION NAME AND ADDRESS: Materials Laboratory (AFWAL/MLLN) Air Force Wright Aeronautical Laboratories (AFSC) Wright-Patterson Air Force Base, Ohio 45433	10. PROGRAM ELEMENT, PROJECT, TASK AREA & WORK UNIT NUMBERS: 2307P102
11. CONTROLLING OFFICE NAME AND ADDRESS: Materials Laboratory (AFWAL/MLLN) Air Force Wright Aeronautical Laboratories (AFSC) Wright-Patterson Air Force Base, Ohio 45433	12. REPORT DATE: Oct 80
	13. NUMBER OF PAGES: 55
14. MONITORING AGENCY NAME & ADDRESS (if different from Controlling Office)	15. SECURITY CLASS. (of this report): UNCLASSIFIED
	15a. DECLASSIFICATION/DOWNGRADING SCHEDULE:

16. DISTRIBUTION STATEMENT (of this Report)

Approved for public release; distribution unlimited.

17. DISTRIBUTION STATEMENT (of the abstract entered in Block 20, if different from Report)

18. SUPPLEMENTARY NOTES

19. KEY WORDS (Continue on reverse side if necessary and identify by block number)

Strain Rate
Hopkinson Bar
Dynamic Properties of Materials
Structural Materials

20. ABSTRACT (Continue on reverse side if necessary and identify by block number)

Stress-strain curves in tension obtained on a large number of structural materials at strain rates up to $10^3 s^{-1}$ are presented. A modified split Hopkinson bar apparatus used for high strain rate tensile testing is described. Data are compared with other published results. The flow stress of all the materials tested is seen to increase to some extent over the range in strain rates from ~~10^{-3} to $10^3 s^{-1}$~~ 0.001 to 10³ c/s.

DD FORM 1 JAN 73 1473 EDITION OF 1 NOV 65 IS OBSOLETE

SECURITY CLASSIFICATION OF THIS PAGE (When Data Entered)

312 662

FOREWORD

This technical report was prepared by the Metals Behavior Branch, Metals and Ceramics Division, Materials Laboratory, Air Force Wright Aeronautical Laboratories. The work was performed by Dr. T. Nicholas, (AFWAL/MLLN) under in-house Project No. 2307P1. The report covers work conducted over a period of over eight years up through December 1979, and was submitted by the author in February 1980.

The author would like to express his deep appreciation to Mr. Jim Paine, Systems Research Laboratories, Dayton, Ohio for his significant contributions in all phases of the experimental program over an extended period of time.

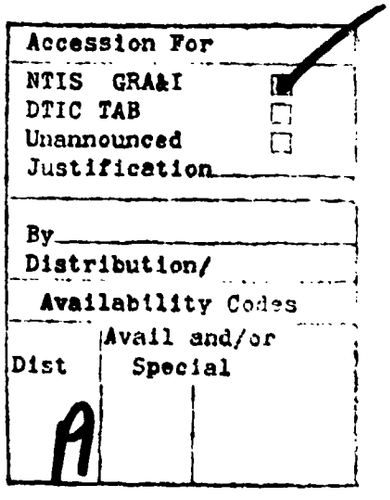

TABLE OF CONTENTS

LIST OF ILLUSTRATIONS

LIST OF ILLUSTRATIONS (CONCLUDED)

LIST OF TABLES

SECTION I

INTRODUCTION

Numerous applications of structural materials involve or impact types of loading. In order to design or analyze dynamically loaded structures more accurately, it is necessary to know the mechanical properties of the materials involved at the strain rates to which the structural components are subjected. It is well known that the mechanical properties of most materials are influenced to some extent by strain rate. The magnitude of such strain rate effects, especially in metals, has been a topic of numerous researchers since the 1950's. Progress in this area has been hampered, however, by the lack of reliable test techniques for determining the mechanical properties of materials at high strain rates. One of the major breakthroughs in this area was the development of the Kolsky apparatus or split Hopkinson bar for high strain rate compression testing (Reference 1). In this technique, a small cylindrical specimen is sandwiched between two long bars. A compression pulse, generated by impact from a third bar or some type of explosive detonation, propagates down one of the long bars and through the specimen into the second bar. The bars remain elastic, although the specimen is deformed into the inelastic region because of the impedance mismatch. The equations of elastic wave propagation in long rods along with the recorded strain gage signals from the two bars are used to determine the time history of both force and displacement at the ends of the rods contacting the specimen. Subject to the assumptions and limitations of the technique (Reference 2), dynamic stress-strain curves in compression can be obtained at strain rates exceeding $10^3 s^{-1}$.

Over a period of several decades, a number of investigators have reported data on compressive high strain rate properties of a variety of materials using this technique (References 3, 4, and 5). There have also been several attempts to generate high strain rate tensile properties using modifications of the Kolsky apparatus. Lindholm and Yeakley (Reference 6) utilized a complex hat type specimen which is really a set of four very small tensile bars in parallel. They used two Hopkinson bars as in the compression test, but one was a solid bar

while the other was a hollow tube having the same cross sectional area. Christman, et al. (Reference 7) used another modification of the Kolsky apparatus in which a compressive pulse was generated in a hollow tube which was attached to a solid inner rod by a mechanical joint. The compressive pulse reflected at the free end through the joint and returned as a tensile pulse through the solid inner rod. A threaded specimen attached to the solid inner Hopkinson bars achieved the tensile equivalent of the Kolsky apparatus for compression and the test was analyzed in the same manner as for the compression split Hopkinson bar. A similar setup was described earlier by Hauser (Reference 8). Harding, Wood, and Campbell (Reference 9) appear to be one of the first to demonstrate this technique for high rate tensile testing. Strain rates of over 1000 s^{-1} were achieved in an apparatus where loading eccentricity is minimized and stress accuracy of ± 5 per cent is achieved. Although these are relatively simple and direct methods for generating high rate tensile data, they suffer from the ability to generate tensile waves having very short rise times because of the wave dispersion at a mechanical joint. More recently, Albertini and Montagnani (Reference 10) utilized both an explosive loading device and rapid fracture of a clamp in a prestressed bar to generate tensile pulses in a split Hopkinson bar apparatus using a threaded specimen and achieved rise times of approximately 25 μs. The Materials Laboratory has been involved in investigations of the dynamic behavior of materials for over a decade. As a part of this program, a tensile version of a split Hopkinson bar was developed and utilized for evaluating the dynamic tensile properties of several grades of beryllium (Reference 11). Over an extended period of time, numerous structural materials have been evaluated in tension at high rates of strain utilizing that apparatus and subsequent modifications. This report is a compilation of data generated over a number of years on various materials. Dynamic stress-strain data were obtained at strain rates up to $10^3 s^{-1}$. A complete description of the apparatus and a discussion of its use and limitations is included for completeness.

SECTION II

APPARATUS AND INSTRUMENTATION

The apparatus consists principally of a striker bar and two Hopkinson pressure bars mounted and aligned on a rigid base as shown schematically in Figure 1. Bar No. 1 is twice the length of bar No. 2, while the striker bar is less than half the length of bar No. 2. In the experiments reported here 0.5" diameter (12.7 mm) AISI 4130 steel bars of lengths 2.5, 6, and 12 feet (.06, .15, and .30 m) were used. The ends of each bar were heat treated to a hardness of $R_{C_1}47$. Figure 2 is a Lagrangian x-t diagram which shows the details of the wave propagation in the bars and indicates how the experiment is performed. The striker bar is accelerated against bar No. 1, the impact generating a compression pulse whose amplitude depends on the striker velocity and whose length is twice the longitudinal elastic wave transit time in the striker bar. The pulse travels down the bar until it reaches the specimen. The threaded tensile specimen of Figure 3 is attached to the two pressure bars as shown in detail "A" of Figure 1. After the specimen has been screwed into the two bars, a split shoulder is placed over the specimen and the specimen is screwed in until the pressure bars are snug against the shoulder. The shoulder is made of the same material as the pressure bars, has the same outer diameter of 0.5" 12.7 mm), and has an inner diameter just sufficient to clear the specimen of .25" (6.4 mm). The ratio of the cross-sectional area of the shoulder to that of the pressure bars is 3:4 while the ratio of the area of the shoulder to the net cross-sectional area of the specimen is 12:1. The compression pulse travels through the composite cross-section of shoulder and specimen in an essentially undispersed manner. The tightening of the specimen by twisting the pressure bars, the relatively loose fit of the threaded joint of the specimen into the bars, and the large area ratio of shoulder to specimen all help to insure that no compression beyond the elastic limit is transmitted to the specimen. In effect, the entire compression pulse passes through the supporting shoulder as if the specimen were not present. Referring again to Figure 2, the compression pulse continues to propagate until it reaches the free end of bar No. 2. There, it reflects and propagates back as a

tensile pulse, shown as ε_i, as it passes gage No. 2. The tensile pulse, upon reaching the specimen at point A, is partially transmitted through the specimen (ε_t) and partially reflected back into bar No. 2 (ε_r). Note that the shoulder, which carried the entire compressive pulse around the specimen, is unable to support any tensile loads because it is not fastened in any manner to the bars.

In performing the experiments, a tight fitting nylon cylinder or collar, approximately 6" (150 mm) long, is slipped over the split shoulder around the specimen and the two ends of the Hopkinson bars to insure accurate axial alignment. In all of the Hopkinson bar tests where specimens were loaded to failure, the failure was always within the gage section, generally within one diameter of the center of the specimen. No failures were experienced at the fillet radii of the specimen or in the threaded section.

The experimental setup at the instant the tensile pulse is reflected from the free end and starts to propagate back down the bar is identical to the compression split Hopkinson bar apparatus except for the change in sign of the loading pulse and the use of a threaded joint to attach the specimen as opposed to the use of a cylindrical compression specimen. In essence, the shoulder is no longer there. Referring to the incident tensile pulse as ε_i, the pulse transmitted through the specimen and down bar No. 1 as ε_t and the reflected pulse ε_r, the Hopkinson bar equations are identical to those of the compression test (References 2 and 3).

$$u_s = -2c \int_0^t \varepsilon_r dt \qquad (1)$$

$$F_s = EA\varepsilon_t \qquad (2)$$

where u_s is displacement in the specimen, F_s specimen force, c the longitudinal wave speed in the bar, E Young's modulus, and A the cross-sectional area of the pressure bar.

The strain gage bridge on bar No. 2 is located at the center of that bar while the gages on bar No. 1 are at the quarter point, precisely equidistant from the specimen as gage No. 2. In this manner, the transmitted and reflected pulses are time coincident (see Figure 2).

The striker and pressure bar lengths have been chosen so that no spurious reflections interfere with the three pulses being recorded during the experiment (ε_i, ε_r, and ε_t). Referring again to the wave diagram of Figure 2, it can be seen that the entire compression pulse traveling down the bars due to the striker bar impact has passed gage No. 2 before the tensile pulse, ε_i, arrives at the gage. In a similar manner, the complete incident pulse, ε_i, passes the gage before the reflected pulse, ε_r, arrives. The first pressure bar has been chosen very long to avoid any strain gage signals due to possible small wave reflections from the shoulder and specimen interface interfering with the recording of the transmitted pulse, ε_t, with gage No. 1. That possible reflection is shown as a dashed line in the wave diagram. The entire tensile loading of the specimen takes place between points A and B in the wave diagram.

The two pressure bars are each instrumented with two active arm strain gage bridges, to cancel bending, which are powered by a stable DC power supply. The three pulses, ε_i, ε_r, and ε_t, are recorded on a dual-beam oscilloscope by delaying the second beam with respect to the first by an amount equal to the wave transit time between the strain gage bridges. The two traces, ε_r and ε_t, which are time coincident by virtue of the placement of the gages equidistant from the specimen, are recorded by using the chopped mode of the oscilloscope preamplifier. A typical set of strain gage traces is shown in Figure 4a.

An X-Y oscilloscope is used to record directly a load-displacement curve. The signal from gage No. 2 is electronically integrated using the circuit diagramed in Figure 5 and fed to the X axis of the oscilloscope. The signal from the other gage, proportional to load in the specimen, is fed to the Y axis. Displacement rate is proportional to the reflected pulse, ε_r, and is obtained from the dual-beam oscilloscope trace by virtue of Equation 1. A typical X-Y photo is shown in Figure 4b.

The strain gage bridges each consist of two active elements placed diametrically opposite to cancel bending waves should any be present. Strain gage calibration is performed by measuring the velocity of the striker bar and recording the signal from the resulting pulse on both strain gage bridges. Since the striker and pressure bars are of the same material and same cross-section, the resulting strain amplitude due to a striker velocity v is

$$\varepsilon = \frac{v}{2c} \qquad (3)$$

The longitudinal wave velocity, c, is obtained experimentally by accurately measuring the wave transit time in the bar as a pulse reflects back and forth using a time mark generator for the time base measurement. Density is also determined experimentally, and Young's modulus is calculated from

$$E = \rho c^2 \qquad (4)$$

The horizontal axis of the X-Y oscilloscope, which records the time-integral of the strain pulse from gage No. 2, is also calibrated dynamically by sending a pulse of known amplitude and time duration down the bars. The amplitude is determined from the measured striker velocity from Equation 3; the time duration is twice the wave transit time in the striker bar.

All data were recorded on Polaroid film from the two oscilloscope displays and reduced digitally with the aid of a Hewlett Packard Model 9820 calculator, digitizer, and plotter system.

SECTION III

MATERIALS AND EXPERIMENTS

A number of materials were tested from various sources. The materials, source, and heat treatment are summarized in Table 1. The information is not complete because many of the materials were furnished in order to obtain dynamic stress-strain data for specific applications or programs and complete information regarding the source or history of the material was not available. In every case, however, test specimens were machined from a single piece of stock.

The specimens were machined in accordance with the dimensions, tolerances, and specifications of Figure 3. At the beginning of the program several specimens of different materials were strain gaged with a 0.062" (1.6 mm) length gage and tested quasi-statically to failure. In addition to load-strain and load-deflection recordings on X-Y plotters, a deflection-strain plot was obtained in each case. The deflection-strain plots were compared for the different materials and found to be nearly identical. Several least-square fitting attempts resulted in obtaining an equation

$$\epsilon = .2658 - .5(1 - \exp^{-.558}) \qquad (5)$$

which closely represents all the strain-deflection data obtained on the variety of materials tested. In this equation, ϵ represents the strain in percent, and δ represents the deflection in mils (.001") between the grips which are identical in size to the threaded ends of the Hopkinson bars as shown in Figure 1. The strain-deflection relation, represented by Equation 5 above, was used in all subsequent experiments of all strain rates to calculate strain from experimentally observed deflections. In this manner, the tedious task of bonding small strain gages on each sample was eliminated. Since the Hopkinson bar tests provide a load-deflection trace directly, this made it easy to transform the data into stress-strain curves with the aid of a digitizer. It was determined that strains could be obtained to an accuracy of better than ± 5 percent using this procedure for strains up to approximately 0.05. There was no

TABLE 1

MATERIAL CHARACTERIZATION

Material Designation	Source	Heat Treatment
6061-T651 Al	0.5" plate	(b)
7075-T6 Al	1.0" Dia rod	(b)
AISI 1020	(a)	(b)
AISI 4340	0.313" Dia rod	Annealed, Rc 30
AISI 304	0.375" Dia rod	(b)
AISI 321	0.375" x 0.75" bar	(b)
AISI 410	0.5" Dia rod	Annealed
AF 1410	0.5" VIM/VAR plate	(b); Rc 45
300M	(a)	Aged at 900°F, 3 hrs; Rc 54; (c)
RHA	0.375" plate	(b); Rc 33
10 B22	(a)	1625°F, water quench, 800°F temper, 1 hr
A-286	0.25" bar forging	Solution treated 2 hrs at 1650°F, oil quench, Aged at 1325°F, 16 hrs, (c)
Ti 6-4	0.5" bar forging	G.E. Spec C50TF12CL-A; (d)
Ti 6-6-2	0.55" bar forging	Annealed at 1600°F, 4 hrs in argon; (d); Heat treated at 1075°F, 2 hrs in air; (c)
Ti 7-4	0.25" bar forging	Annealed at 1450°F, 1 hr in vacuum, cool to 1050°F at 300°F/hr max., air cool below 1050°F, stress relieved at 1020°F, 2 hrs; (c)
Ti 8-1-1	0.4" bar forging	G.E. Spec C50TF23CL-B; (d)
IN718	(a)	(b)
90-7-3W	(a); No swaging	(b)
DU	(a)	(b)
ETP CU	(a)	Annealed at 1000°F, 1 hr; (c)
S-65 Be	(a)	Etch to remove 0.004" per surface; (c)

(a) Unknown (b) As received (c) After machining (d) Before machining

verification of the strain-deflection curve beyond 0.05 strain because the strain gages peeled off at larger strains in the static tests. Except for very small strains, the strain-deflection curve is linear, corresponding to an effective gage length of approximately 0.38" (9.6 mm) compared to a true gage length of 0.35" (8.9 mm) as shown in Figure 3. The difference is due obviously to the strain contribution of the portion of the specimen outside the points of tangency of the fillet radii and appears quite reasonable.

Quasi-static and intermediate rate tests were run on an MTS servo-controlled hydraulic testing machine over a range of cross-head velocities corresponding to strain rates from approximately 10^{-4} sec^{-1} up to 20 sec^{-1}. Although higher velocities could be achieved with the machine, no meaningful data could be obtained because of inertia effects and load cell ringing. Load was recorded on the MTS load cell while deflection was recorded using an LVDT mounted on a special fixture which was made to hold the specimen in perfect alignment. Load versus deflection was recorded on an X-Y plotter at the lower loading rates and on an X-Y oscilloscope at the higher MTS machine rates. Strain rate was obtained from the (constant) cross-head deflection rate as measured separately with the LVDT output against time using the linear portion of the strain-deflection curve, i.e., an effective gage length of 0.38" (9.6 mm).

High rate, split Hopkinson bar tests were conducted over a range in strain rates of from approximately 10^2 to 10^3 s^{-1} depending on the material and the impact velocity. The lowest strain rate obtainable is governed by the total time available for the test of approximately 300 μs. This is the total time of the loading pulse, which is twice the wave transit time in the striker bar. Since $\varepsilon = \dot{\varepsilon}t$, an average strain rate, $\dot{\varepsilon}$, of 100 s^{-1} for 300 μsec corresponds to a total strain of only 3 percent in the specimen. Since the upper limit of t is fixed in the experiment by the length of the striker bar, continual decreasing of $\dot{\varepsilon}$ will eventually reach a loading condition where failure of the specimen will not be achieved. The upper limit of strain rate of 10^3 s^{-1} was governed by practical considerations including the rise-time of the loading pulse, the maximum pulse amplitude governed by the strength of

the input bars and, most important, the split shoulder configuration. At the highest loading rates, wave reflections and interactions started to obscure the experimental data.

SECTION IV

RESULTS AND DISCUSSION

Stress-strain curves at low, intermediate, and high strain rates are presented in Figures 6 through 25. Each low and intermediate rate curve represents the average of two or three curves obtained under identical conditions. In all cases, the scatter from test to test was essentially negligible and the curves thus represent the actual behavior. For the high rate tests, at least three tests were run for each material at similar strain rates. Again, the scatter from test to test was within several percent. The actual data points are not presented because the digitization of the data provided hundreds of points per test which, when plotted, provided an essentially continuous curve. These curves were superimposed for each rate and traced to obtain the final curves as presented.

For each material, a low strain rate curve at a rate of $4.4 \times 10^{-4} s^{-1}$ is presented and noted as a strain rate of $4 \times 10^{-4} s^{-1}$. Note that in the testing the ram velocity of the machine was kept constant. The actual velocity of the ends of the specimen is somewhat different due to the compliance of the machine and loading attachments. Note further that for small strains the relation between specimen strain and displacement is also non-linear. It is thus misleading to quote specimen strain rate to an accuracy greater than one significant digit. In a similar manner, intermediate rate test data are presented corresponding to a calculated strain rate of $4.4\ s^{-1}$ and labeled as such. Finally, the high rate curves obtained with the Hopkinson bar apparatus are labeled with the average strain rate rounded to the nearest hundred.

The use of a very small specimen to obtain a stress-strain curve and the indirect determination of strain from relative specimen grip displacement measurements makes the accuracy of the strain values no better than ± 5 percent. Furthermore, for very small strains where the strain-displacement relation (Equation 5) is nonlinear, i.e. for strains under 1 percent, the accuracy of the strain calculations is poor. On the other hand, the use of the identical specimen for tests at all strain

rates and the identical manner of calculating strains from grip displacement measurements in each test makes the comparison of data at various strain rates much more reliable. Thus, although the exact shape and magnitude of these quasi-static curves could have been obtained much more accurately, the method used makes direct comparison with the high rate curves more realistic.

The inherent limitations of the split Hopkinson bar method preclude its use for determining material behavior in the elastic region because of stress wave reflections, stress nonuniformity, and large variations in strain rate during the initial portions of the test. The stress-strain data obtained from such a test are thus valid only after some degree of stress and strain rate uniformity is achieved. Figure 26 presents typical data from a test on Ti 6-4. Note that in this test that strain rate is changing rapidly for approximately 25 μs. During this time, a total strain of over 1 percent has been accumulated. A plot of load or stress versus strain, based on time integration of strain rate as obtained from the reflected pulse in the Hopkinson bar, gives an apparent elastic modulus much lower than the known values for titanium. This merely demonstrates that Hopkinson bar data can only be used to obtain flow stress data outside of the elastic region or where the fundamental assumptions of the Hopkinson bar are satisfied. In the curves presented, the elastic region does not represent experimentally obtained data but is drawn merely for completeness from known values to provide realistic stress-strain curves.

Figure 26 also shows the typical variation of strain rate during the Hopkinson bar test. The average value of strain rate for this test is shown dashed and is obtained by eyeball estimate. This illustrates why strain rates are not quoted to better than the nearest hundred in the Hopkinson bar data because strain rate is not constant in this type of test.

For comparison with data of other investigators, the stress-strain curves at various strain rates can be replotted as stress versus log strain rate using yield stress, ultimate stress, or stress at a fixed

value of either total strain or plastic strain. Figure 27 presents such a plot for the three stainless steels tested in this investigation in addition to data of Albertini and Montagnani (Reference 10) for two materials and Hauser (Reference 8), for AISI 304, although the latter were obtained in compression. The data indicates an increase of flow stress with (log) strain rate, with the degree of rate sensitivity increasing at rates of approximately 10 to 10^2 s^{-1}.

Data for the four titanium alloys tested here are presented in Figure 28 along with compression data for Ti 6-4 from Maiden and Green (Reference 4). Again, all the titanium alloys show an increase in flow stress with strain rate with the degree of rate sensitivity apparently increasing slightly at the higher strain rates. Steidel and Makerov (Reference 12), tested a number of titanium alloys over a range of strain rates in tension from 10^{-4} to over 10 s^{-1} and repo. ted data showing an increase in yield stress of approximately 5 ksi (35M Pa) per decade in strain rate. This value is consistent with the data of Figure 28 over the same range in strain rates.

The largest body of data in the literature on strain rate effects deals with pure aluminum and aluminum alloys. Surveys such as those by Lindholm and Bessey (Reference 13) and Jiang and Chen (Reference 14) show that although there is some degree of strain rate dependence in pure aluminum, the higher strength aluminum alloys tend to be strain rate independent over a range in strain rates from approximately 10^{-4} to 10^3 s^{-1}. Most of the data reported, however, were obtained in compressions. Holt, et al. (Reference 5) show essentially no strain rate sensitivity for 6061-T6 and 7075-T6 aluminum in compression up to strain rates of 910 and 560, respectively, using a split Hopkinson bar. Similar results were obtained by Maiden and Green (Reference 4) for the same alloys.

In the data presented in Figures 6 and 7, there appears to be an increase in flow stress at the highest rates tested for both 6061-T651 and 7075-T6 aluminum, although there is no apparent rate sensitivity up to the intermediate rate of 4 s^{-1} in tension. A search of the literature of strain rate effects in those two alloys in tension reveals some interesting

data. For 6061-T6 Al, Smith (Reference 15) found an increase in flow stress at $\varepsilon = .05$ of 15 percent going from a strain rate of 1.7×10^{-4} to 192 s^{-1}. This compares with an increase of 12 percent in our tests at a rate of 600 s^{-1}. Steidel and Makerov (Reference 12) found an increase in flow stress of approximately 5 percent at a rate of 69 s^{-1}, for 6061-T6 Al while Lindholm et al. (Reference 16) report approximately 7 percent increase in yield stress at 10^3 s^{-1} for 6061-T651 Al compared to values at quasi static strain rates. Hoge (Reference 17) shows an increase in yield stress of approximately 28 percent for 6061-T6 Al going from a strain rate of 5×10^{-5} to 65 s^{-1}. Data for yield and ultimate stress in tension from References 12, 15, 17, 18, and 19 have been compiled by Jiang and Chen (Reference 14) for 6061-T6 Al and replotted as Figure 29 which also shows the data from this investigation for $\varepsilon = .04$. Although there is a negligible amount of strain rate sensitivity up to a strain rate of approximately 10 s^{-1}, the degree of rate sensitivity in tension appears to increase for higher strain rates. This same observation is reported by Hoge (Reference 17). Earlier experiments by Harding, Wood, and Campbell (Reference 9) on a high strength aluminum alloy RR77 showed an increase in flow stress of approximately 25 percent over quasi-static values at tensile strain rates of approximately 800 and 1800 s^{-1}. These observations appear to conflict with observations from compressive tests where little or no rate sensitivity is observed in aluminum alloys up to strain rates of approximately 10^3 s^{-1}.

The data of Figure 7 indicate an increase in flow stress of approximately 20 percent for 7075-T6 Al at a rate of 800 s^{-1} compared to the quasi-static data. There are insufficient data in the literature on this alloy for comparison although, as has been noted above, the strain rate sensitivity for this alloy is negligible in compression at similar strain rates.

The data for several grades of steel and some miscellaneous materials are replotted in Figures 30 and 31. Again, it appears that for all of these materials the strain rate sensitivity is increasing at the higher strain rates. The data for S-65 grade beryllium were previously reported (Reference 11) along with the stress-strain curves at various rates and data for two other grades of beryllium which showed similar degrees of strain rate dependence.

SECTION V

CONCLUSIONS

An experimental technique has been developed and demonstrated on over twenty different materials for obtaining high rate stress-strain data in tension at strain rates up to approximately 10^3 s^{-1}. Data have been presented in the form of average stress-strain curves at quasi-static, intermediate, and high rates of strain on a wide variety of structural metals and alloys. The data are compared with those of other investigators and agree favorably. For the aluminum alloys tested here, a small amount of rate sensitivity is observed in tension at the highest strain rates which appears to contradict the findings of others based upon compression test data. An examination of the literature appears to confirm the rate sensitivity findings in tension and raises the question for future investigations of the existence and degree of strain rate sensitivity for high strength aluminum alloys in tension versus compression.

For a broad range of over twenty structural alloys including aluminums, titaniums, and steels, the stress-strain curves over a wide range of strain rates indicate a small amount of strain rate sensitivity with (log) strain rate up to approximately 10 s^{-1} and then a greater degree of rate sensitivity at higher rates of strain.

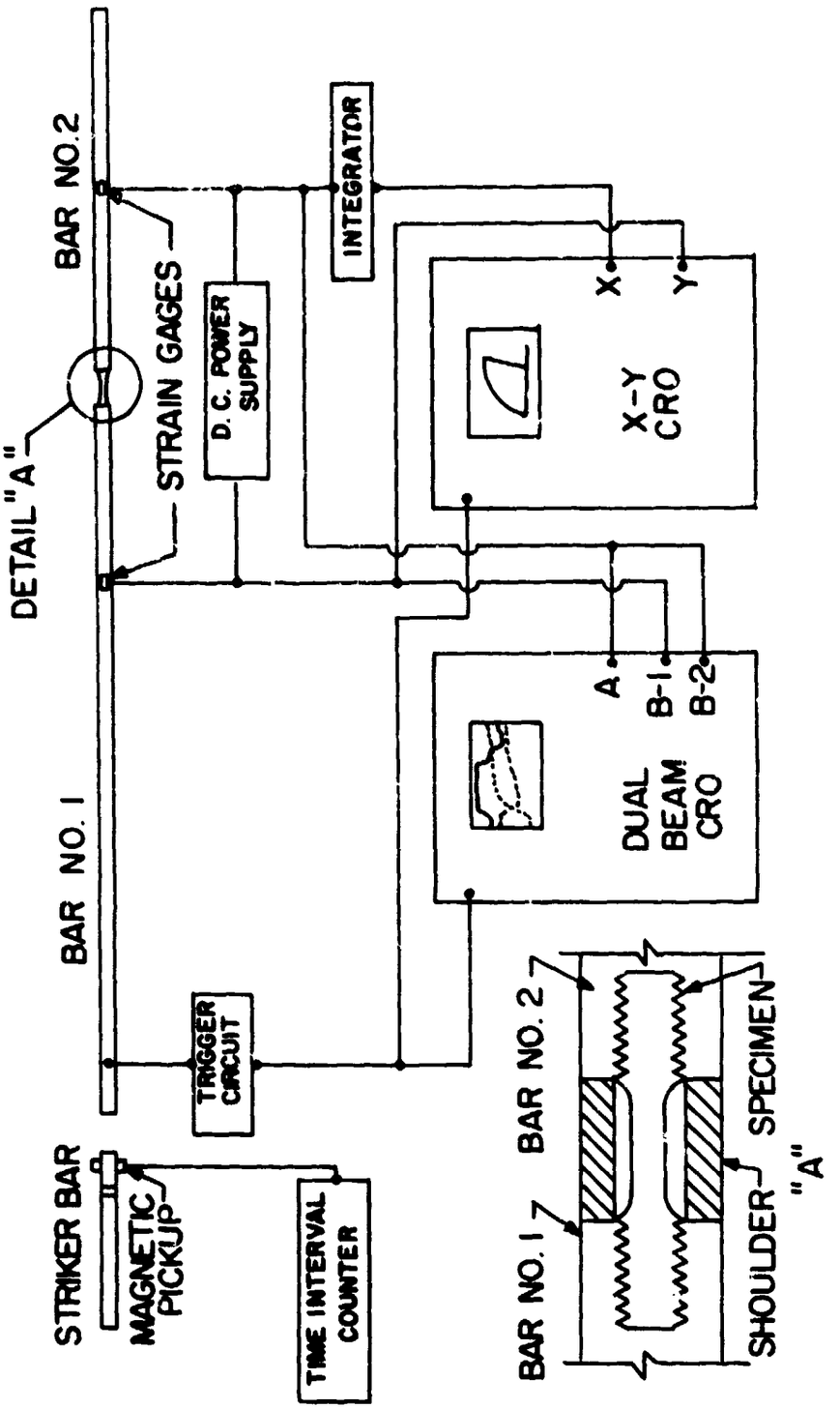

Figure 1. Schematic of Apparatus and Instrumentation

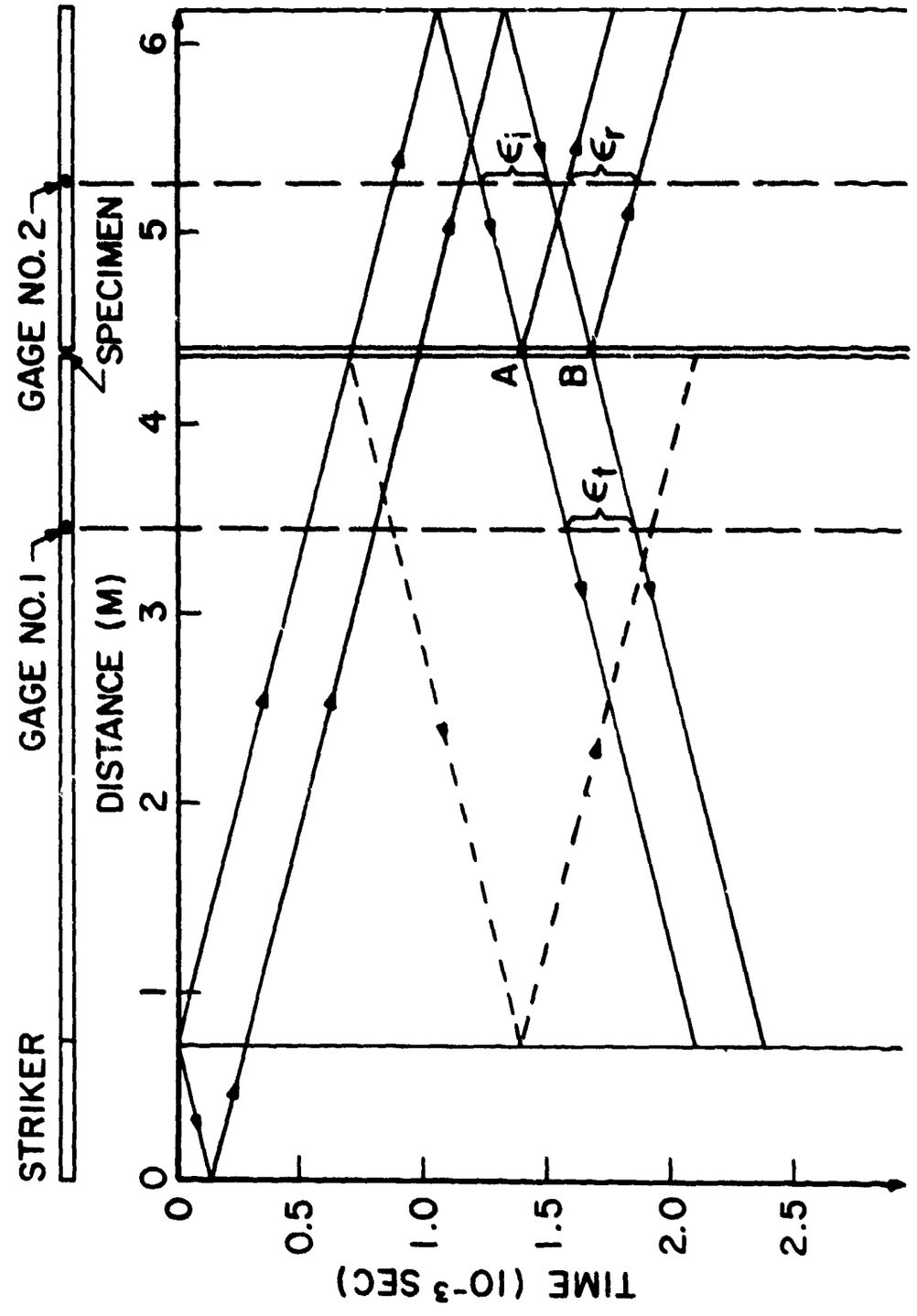

Figure 2. Lagrangian x-t Diagram

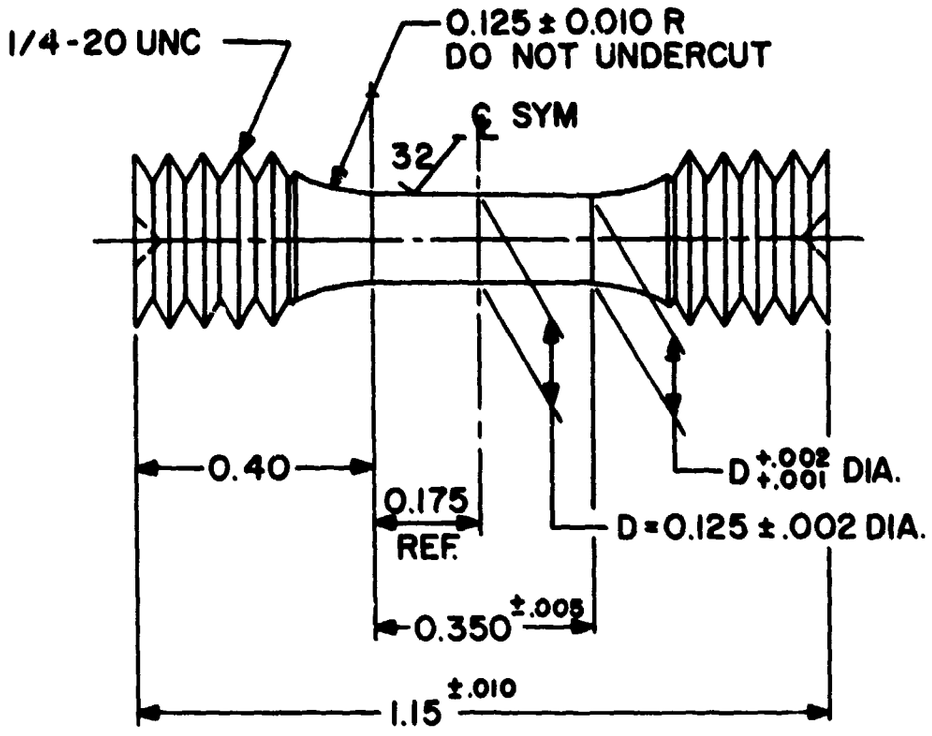

NOTES:

ALL DIMENSIONS IN INCHES

Figure 3. Threaded Tension Hopkinson Bar Specimen

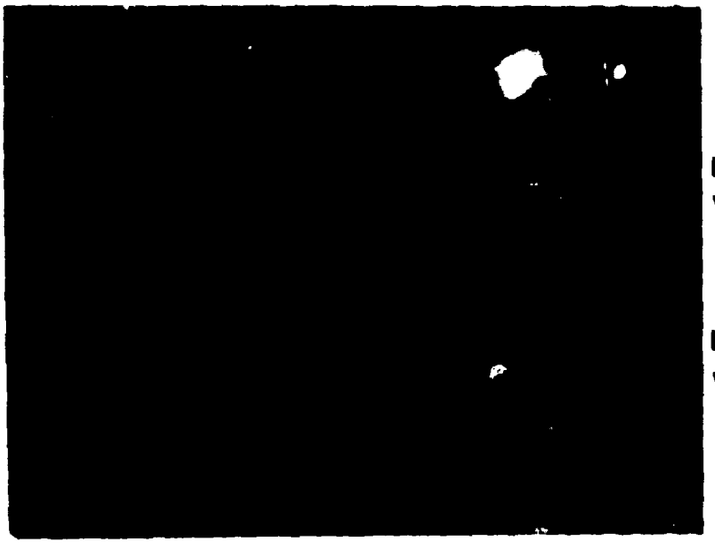

Upper trace
Horiz: 100 μ sec/div
Vert: 6.26×10^{-4}/div

Lower trace
Horiz: 50 μ sec/div
Vert: 1948 lb/div

(a)

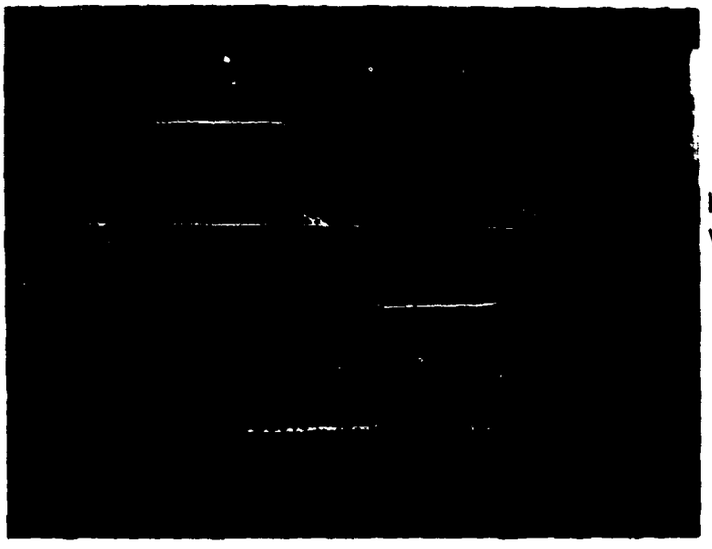

Horiz: 2.31×10^{-2} in/div
Vert: 465 lb/div

(b)

Figure 4. Typical Oscilloscope Traces For AISI 304, Spec. No. 7

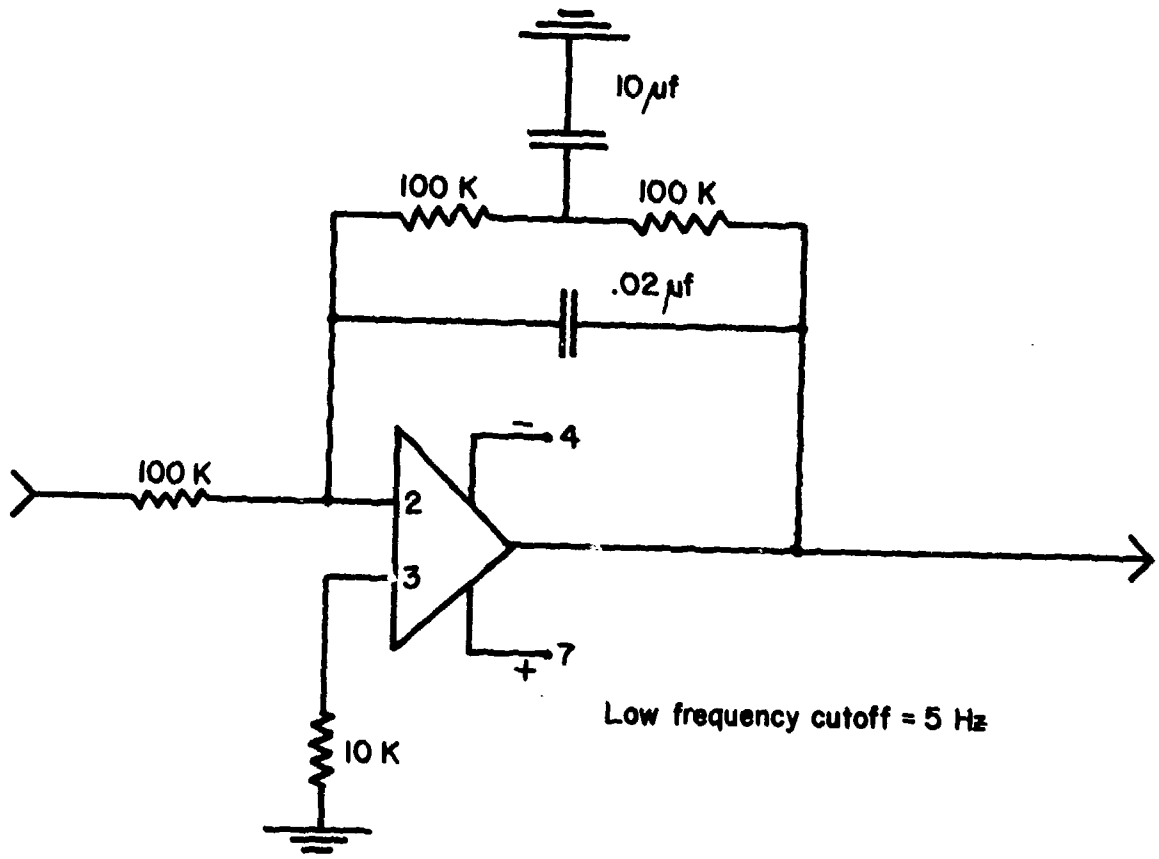

Figure 5. Hopkinson Bar Integrator Circuit

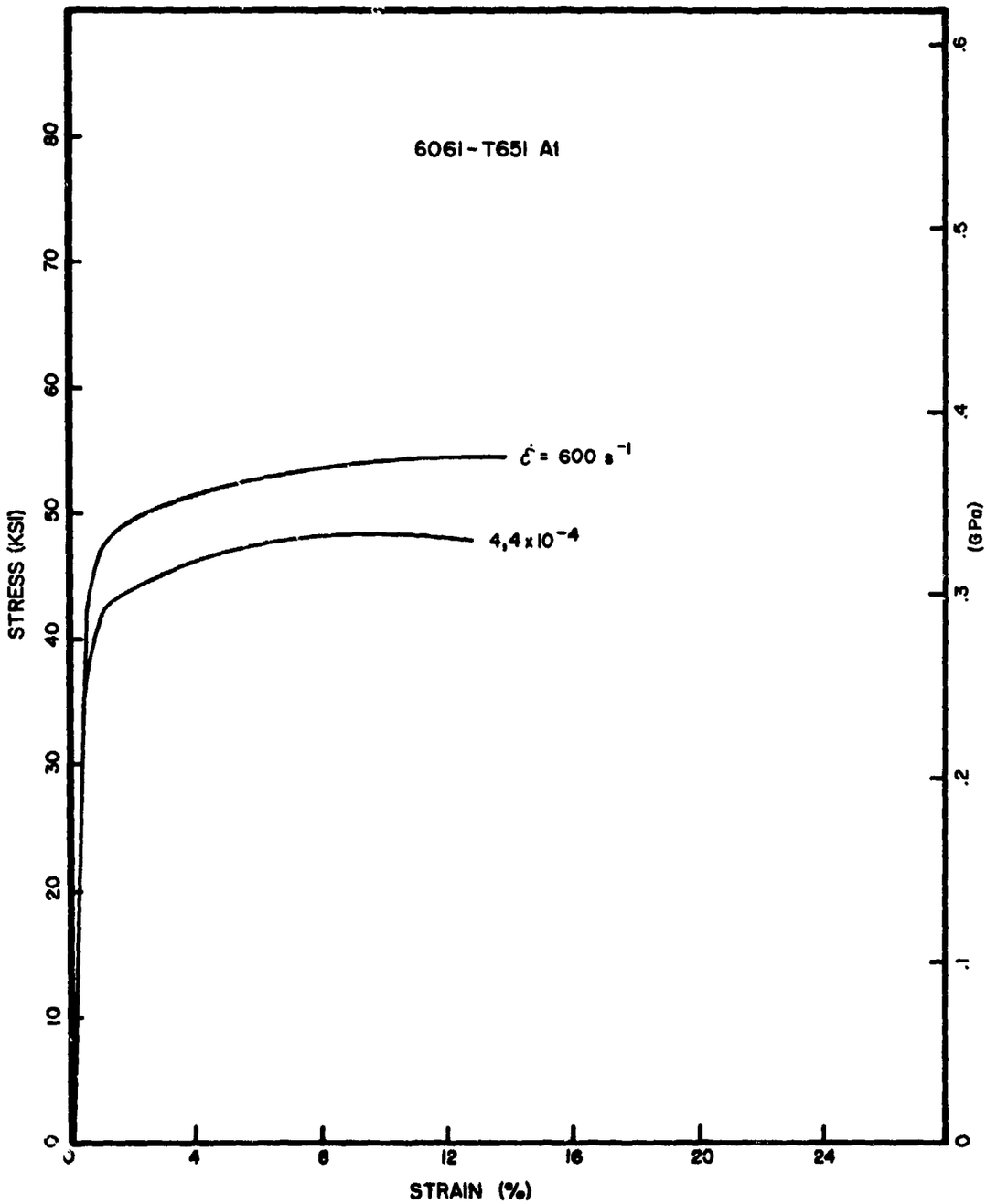

Figure 6. Stress-Strain Curves, 6061-T651 Al

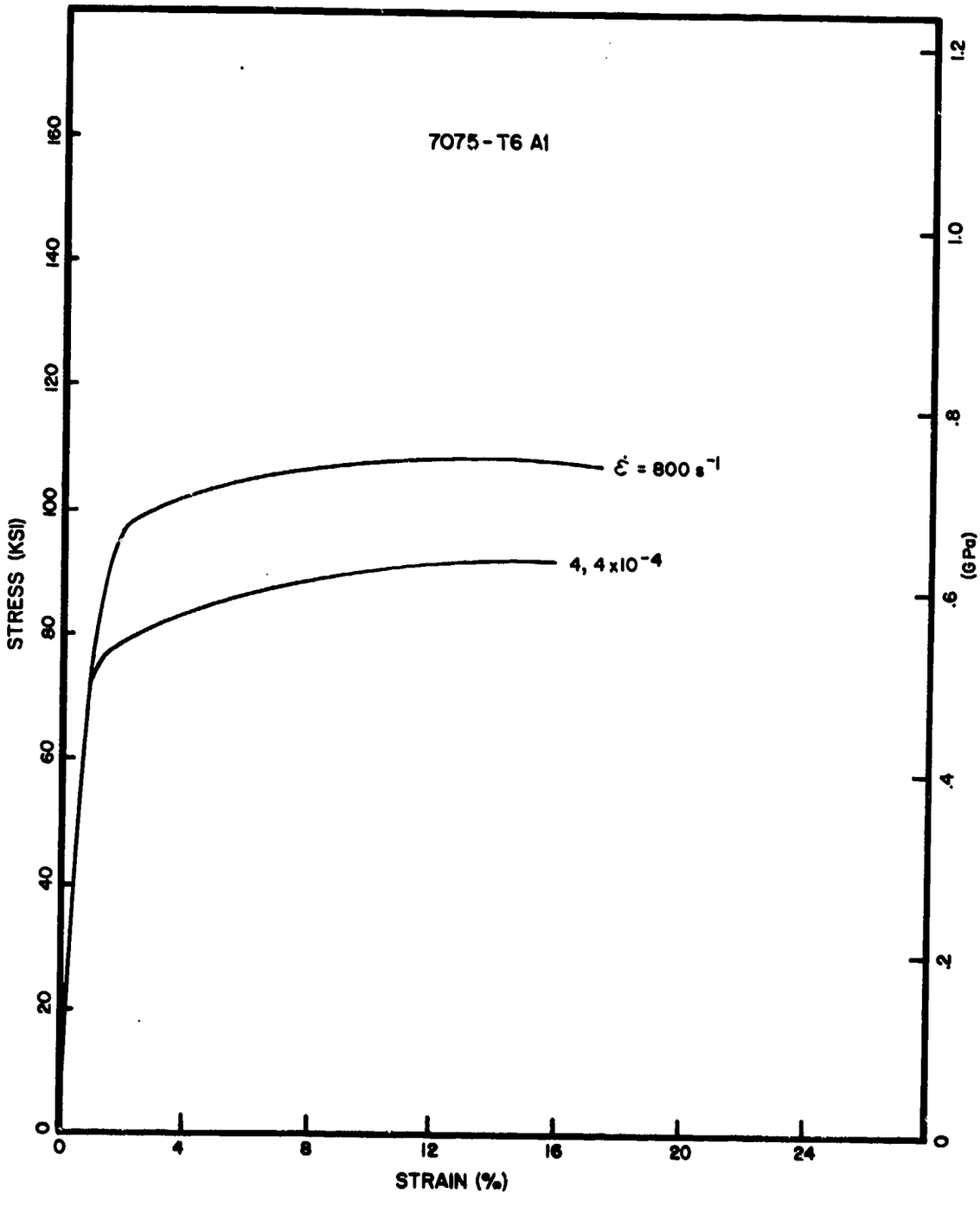

Figure 7. Stress-Strain Curves, 7075-T6 Al

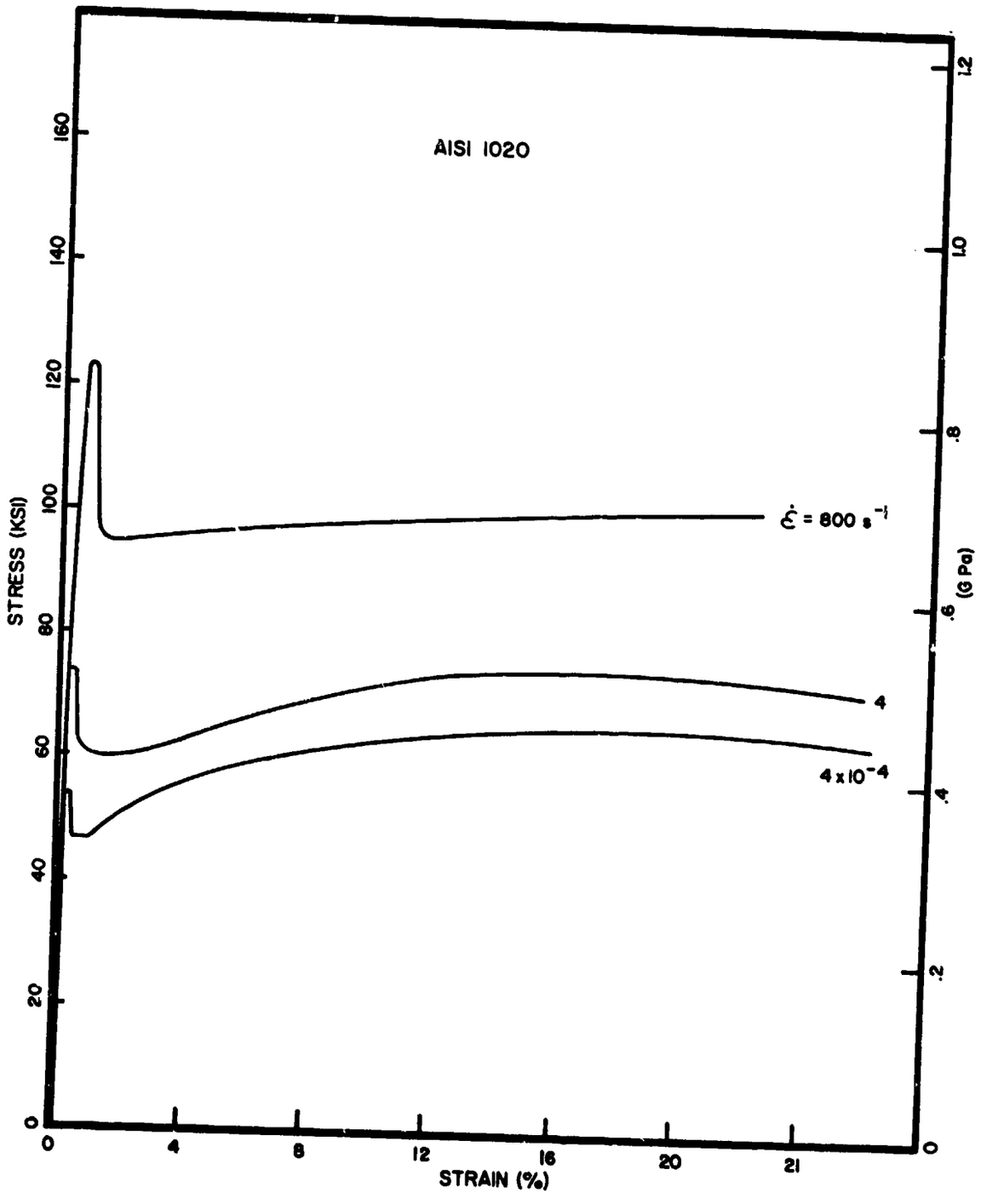

Figure 8. Stress-Strain Curves, AISI 1020 Steel

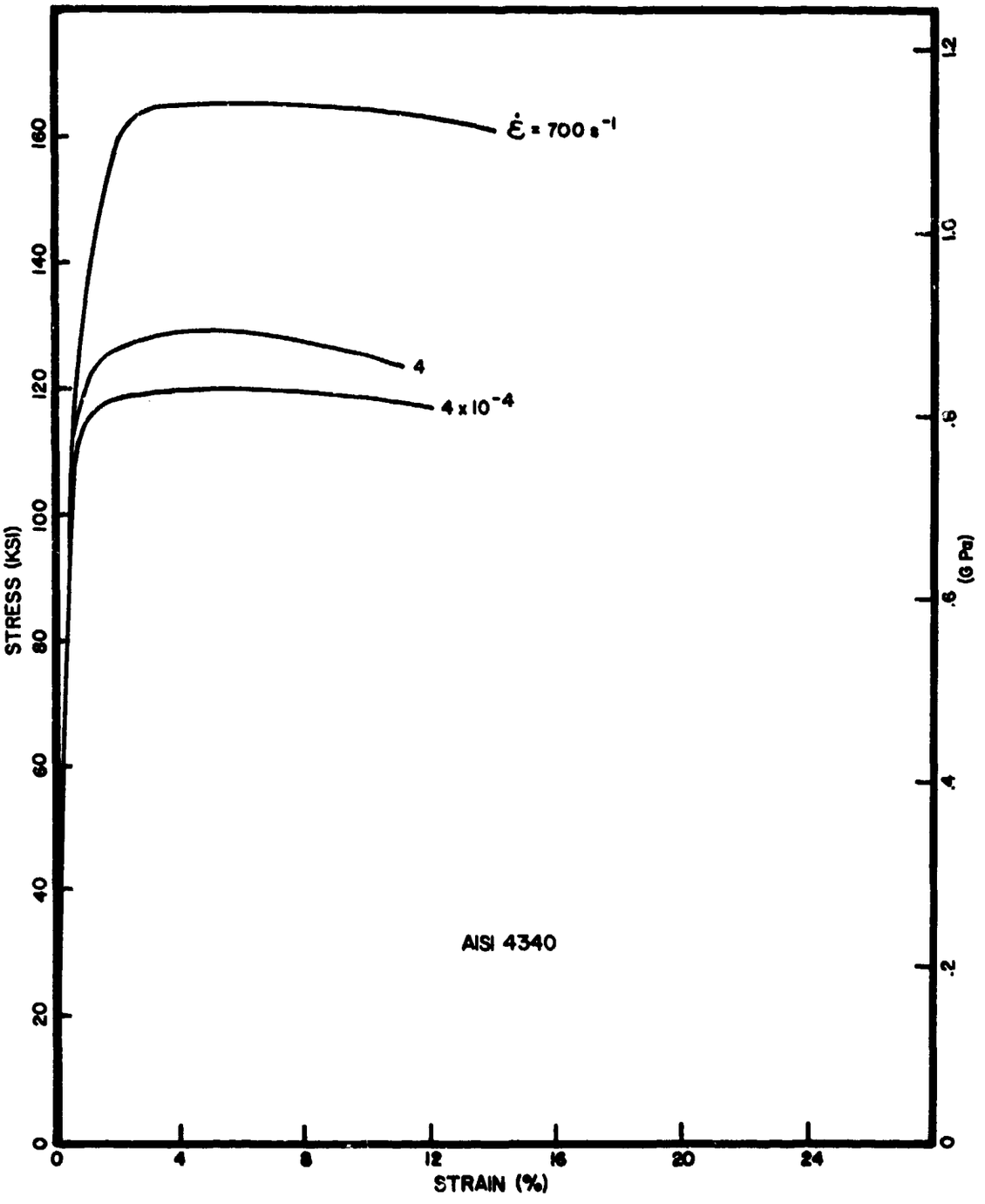

Figure 9. Stress-Strain Curves, AISI 4340 Steel

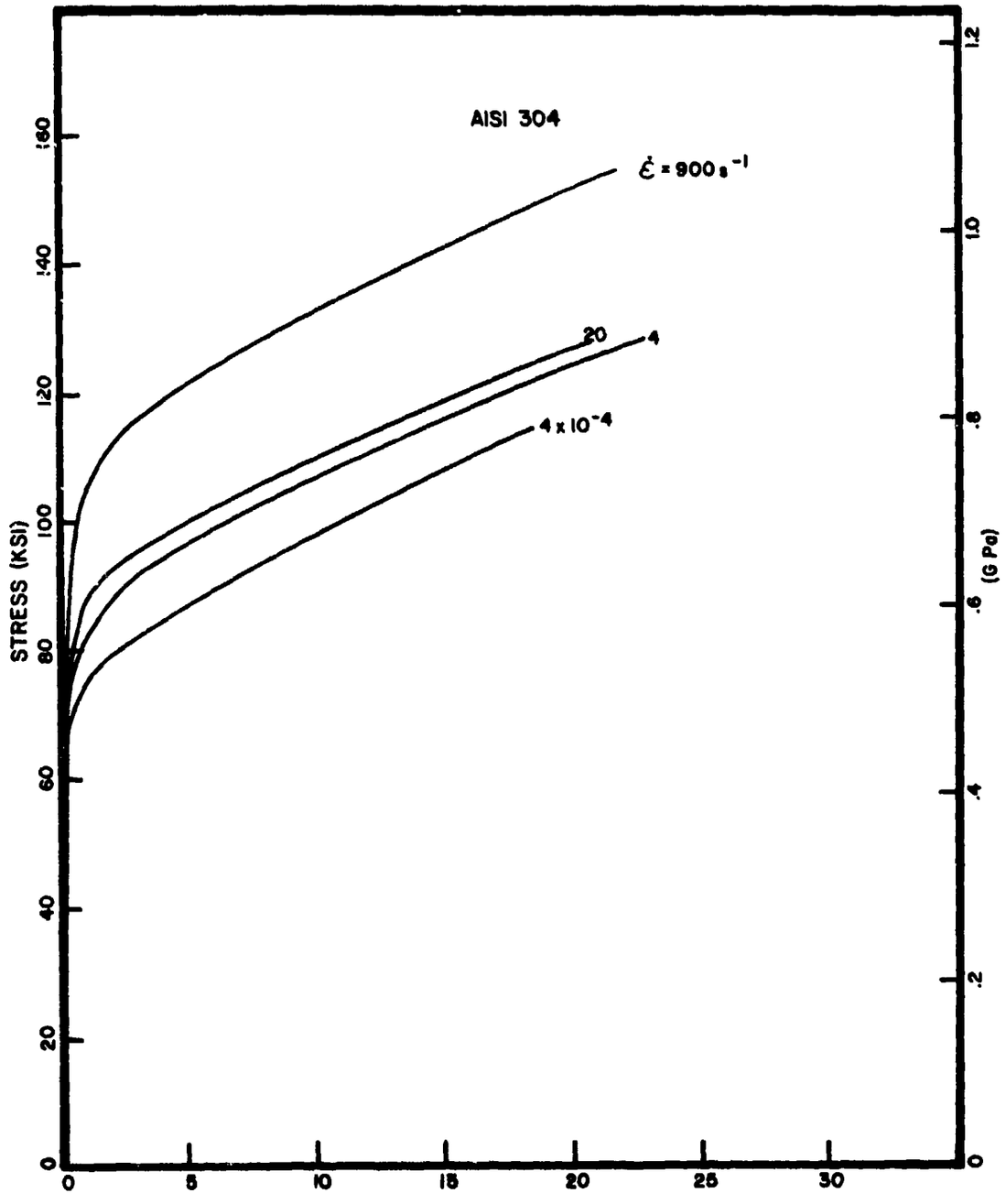

Figure 10. Stress-Strain Curves, AISI 304 Stainless Steel

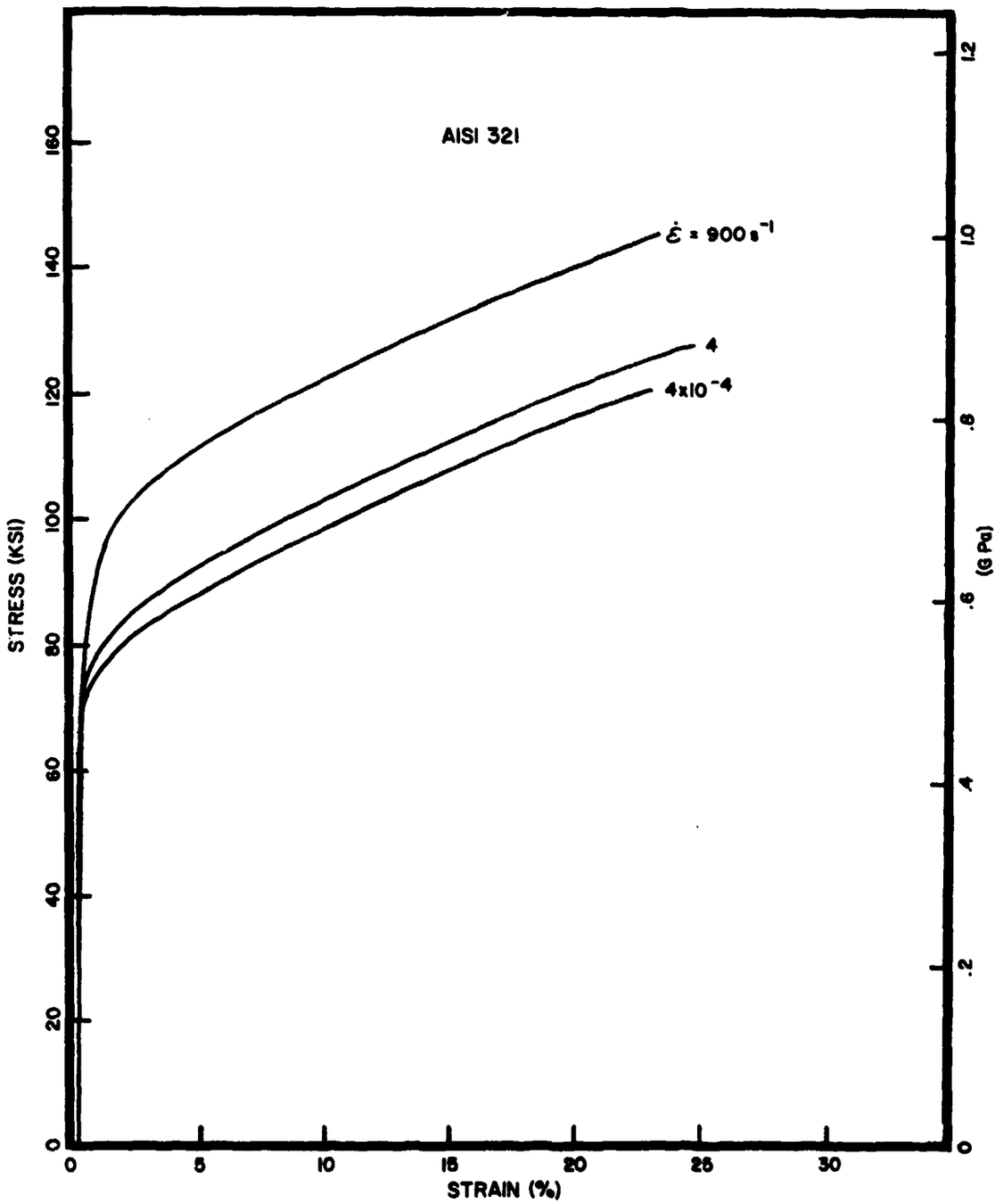

Figure 11. Stress-Strain Curves, AISI 321 Stainless Steel

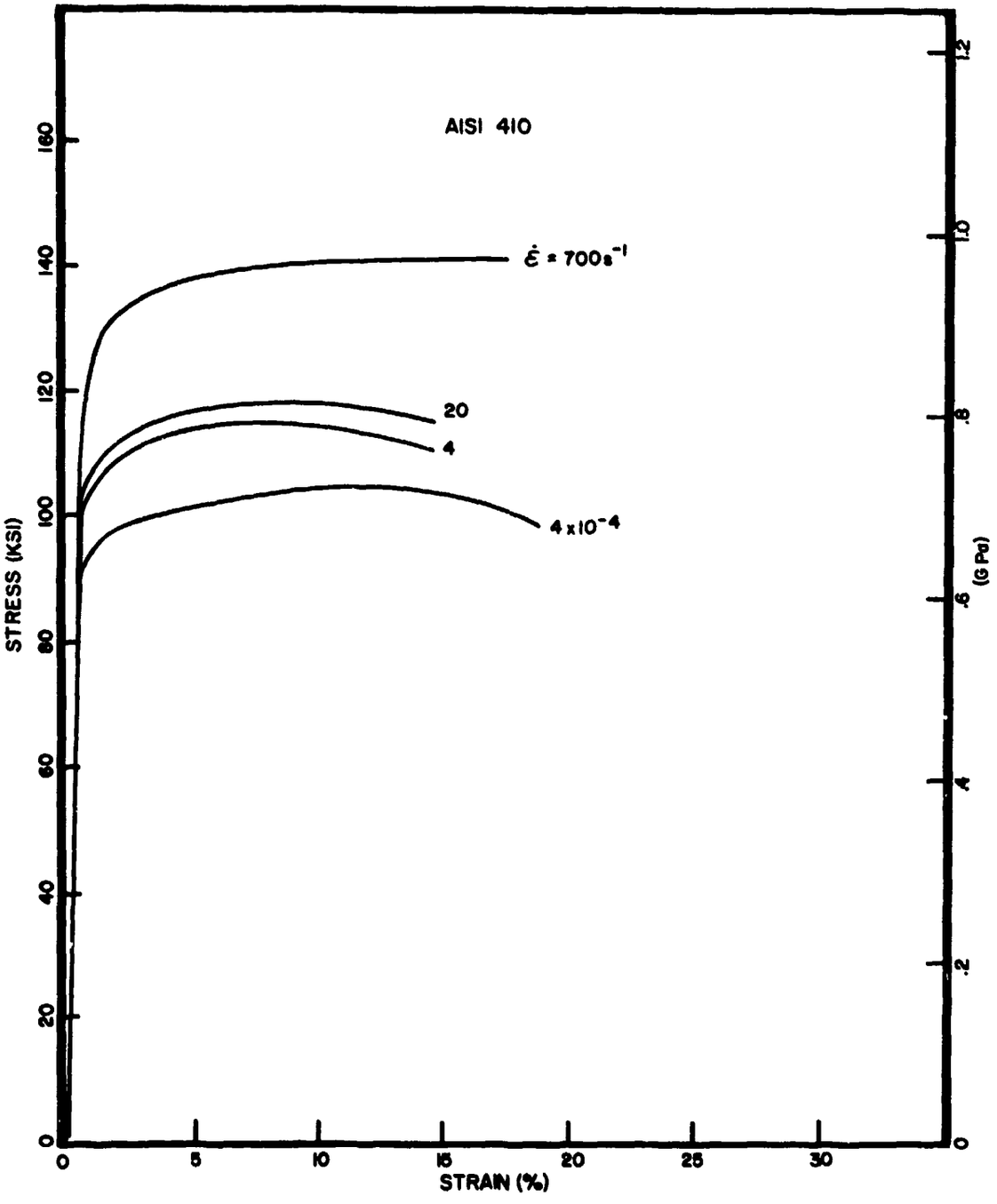

Figure 12. Stress-Strain Curves, AISI 410 Stainless Steel

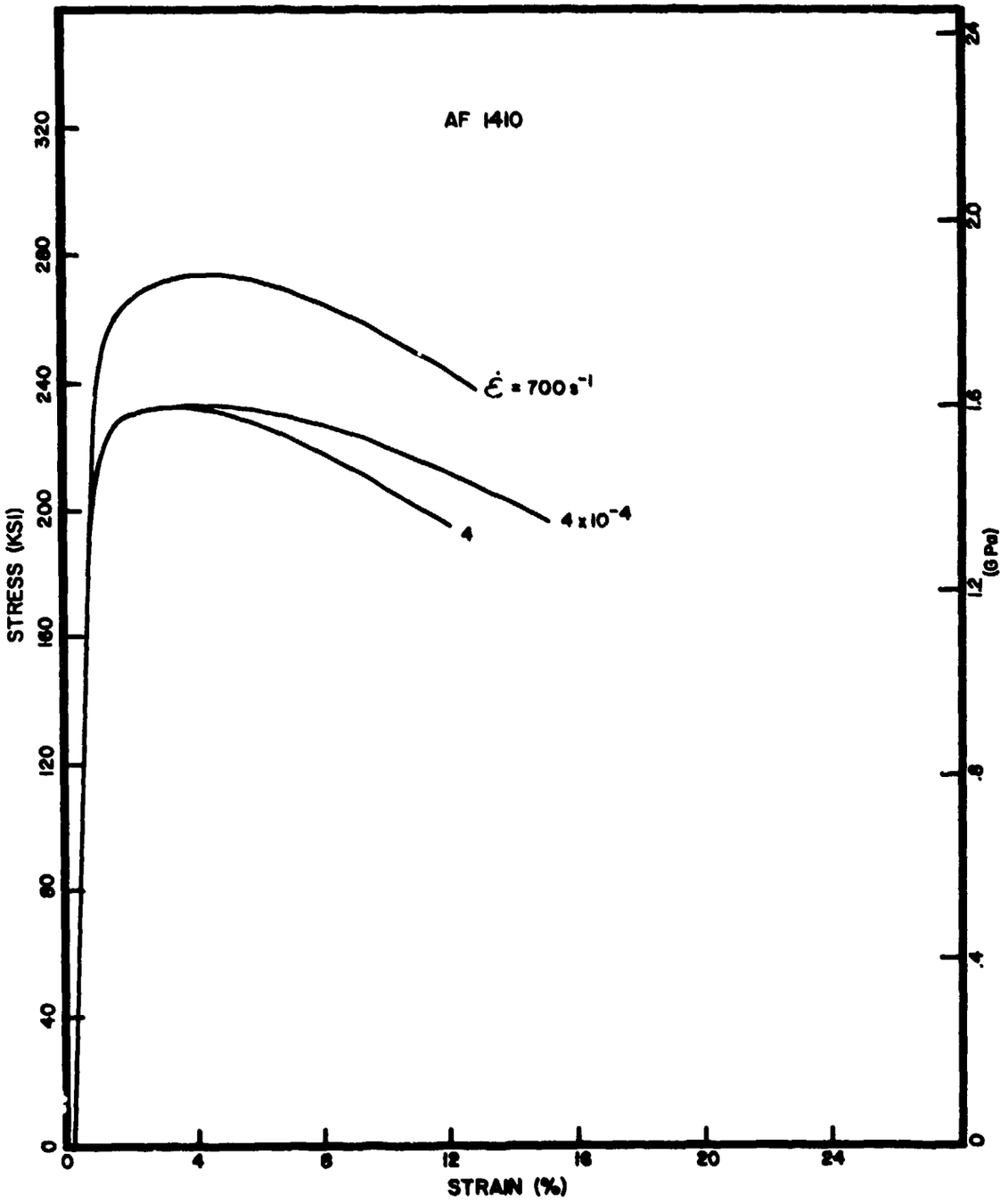

Figure 13. Stress-Strain Curves, AF 1410 (10 Ni Modified Steel)

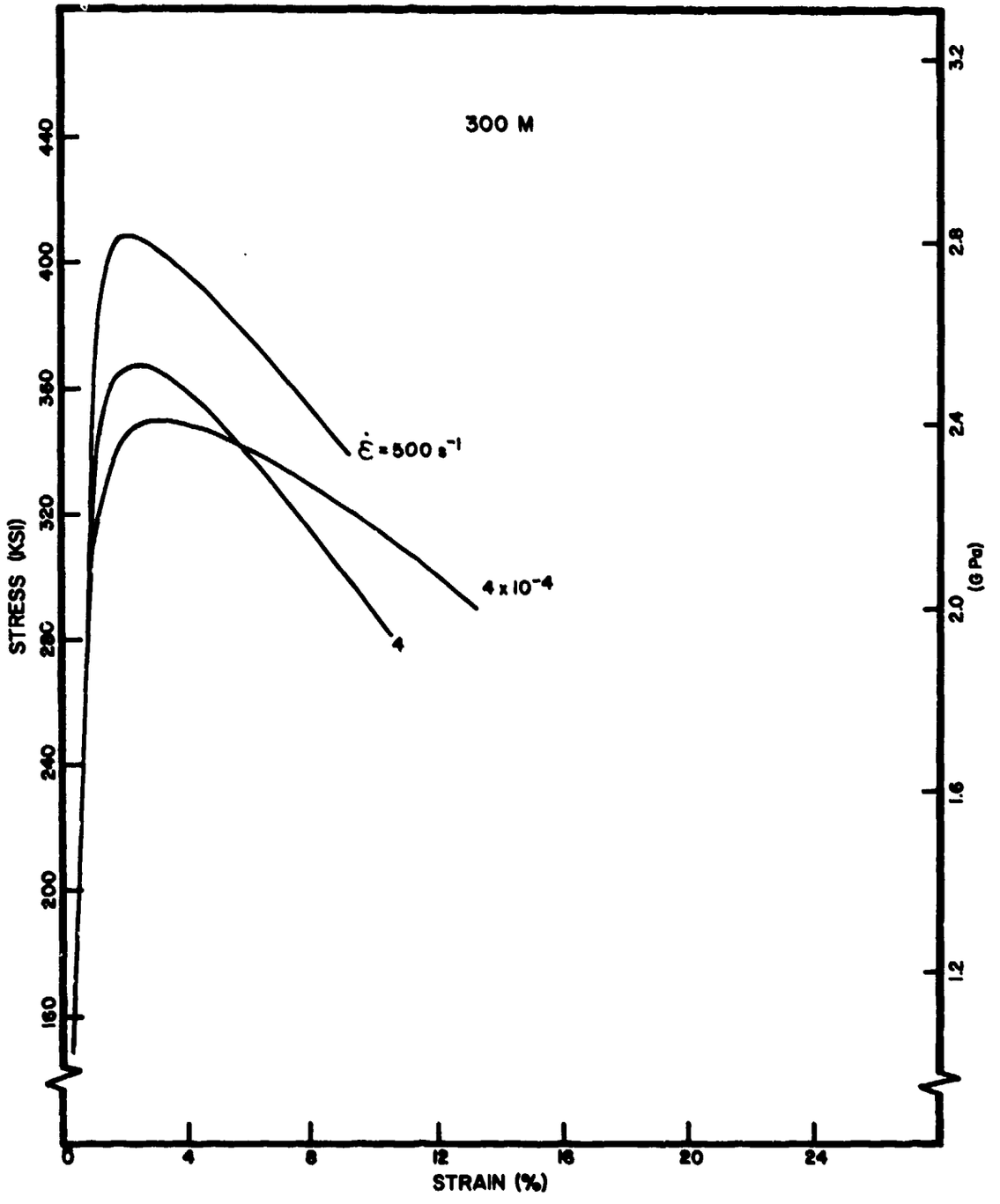

Figure 14. Stress-Strain Curves, 300 M Maraging Steel

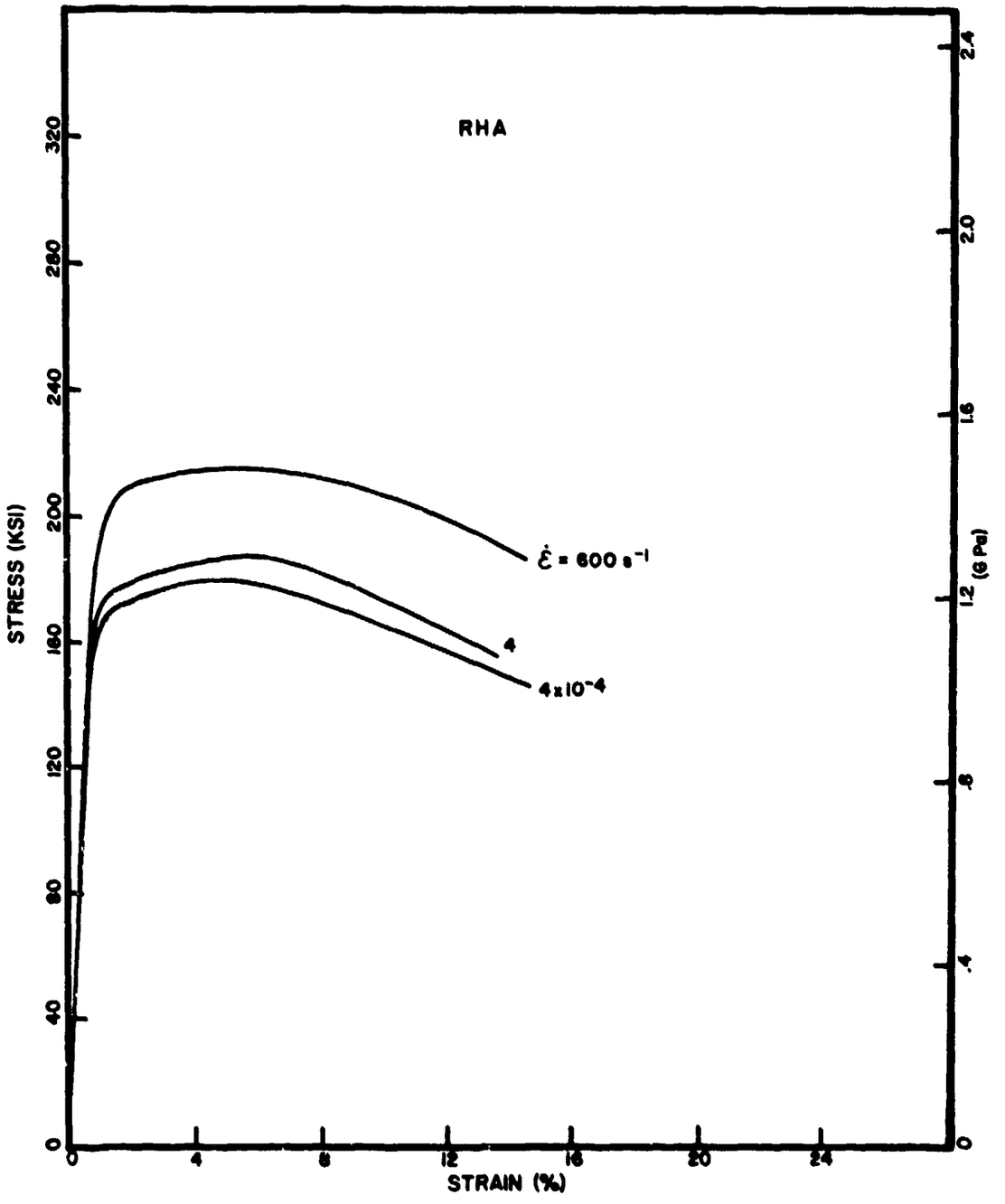

Figure 15. Stress-Strain Curves, RHA (3/8" rolled homogeneous armor plate)

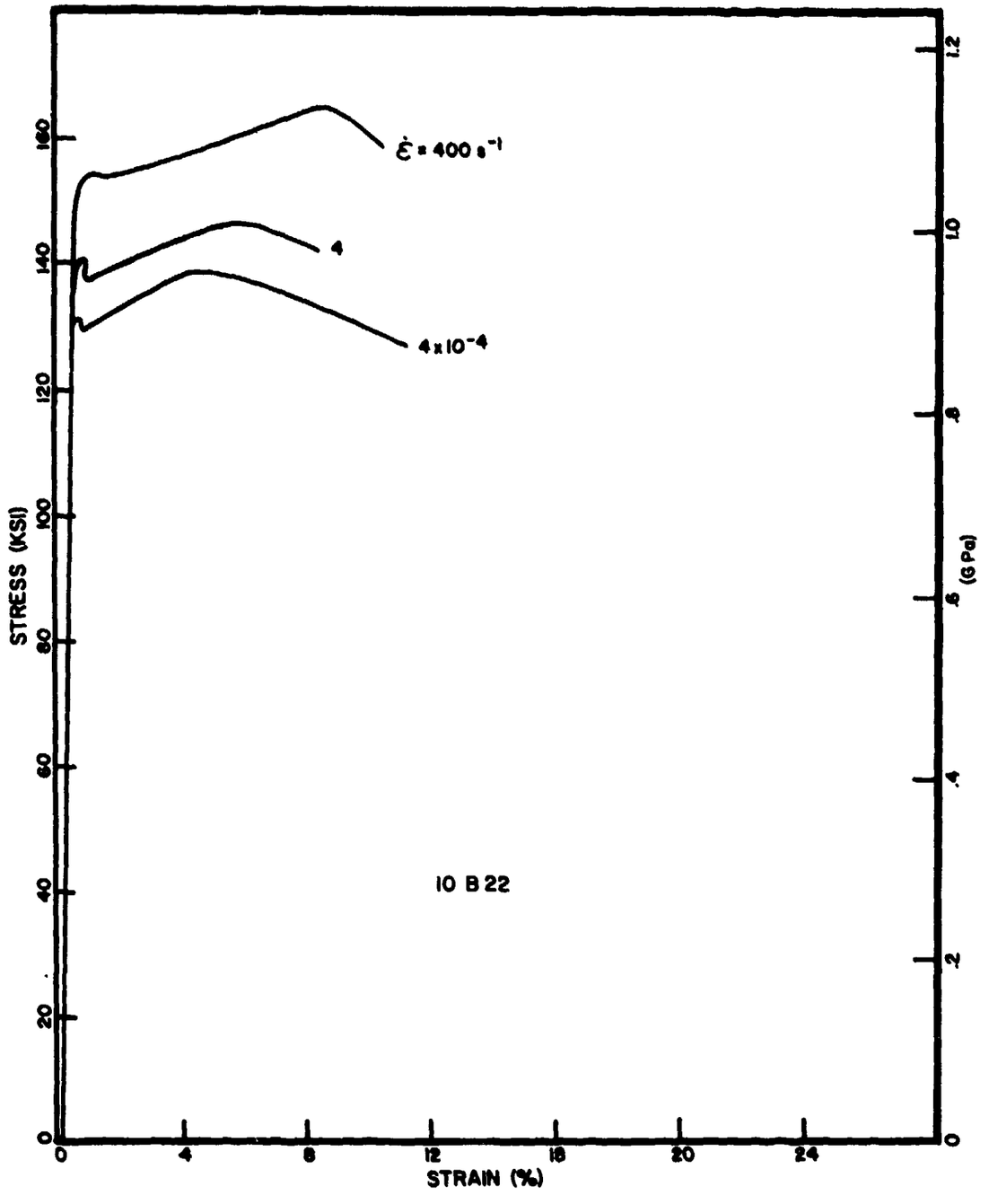

Figure 16. Stress-Strain Curves, 10 B22 Steel

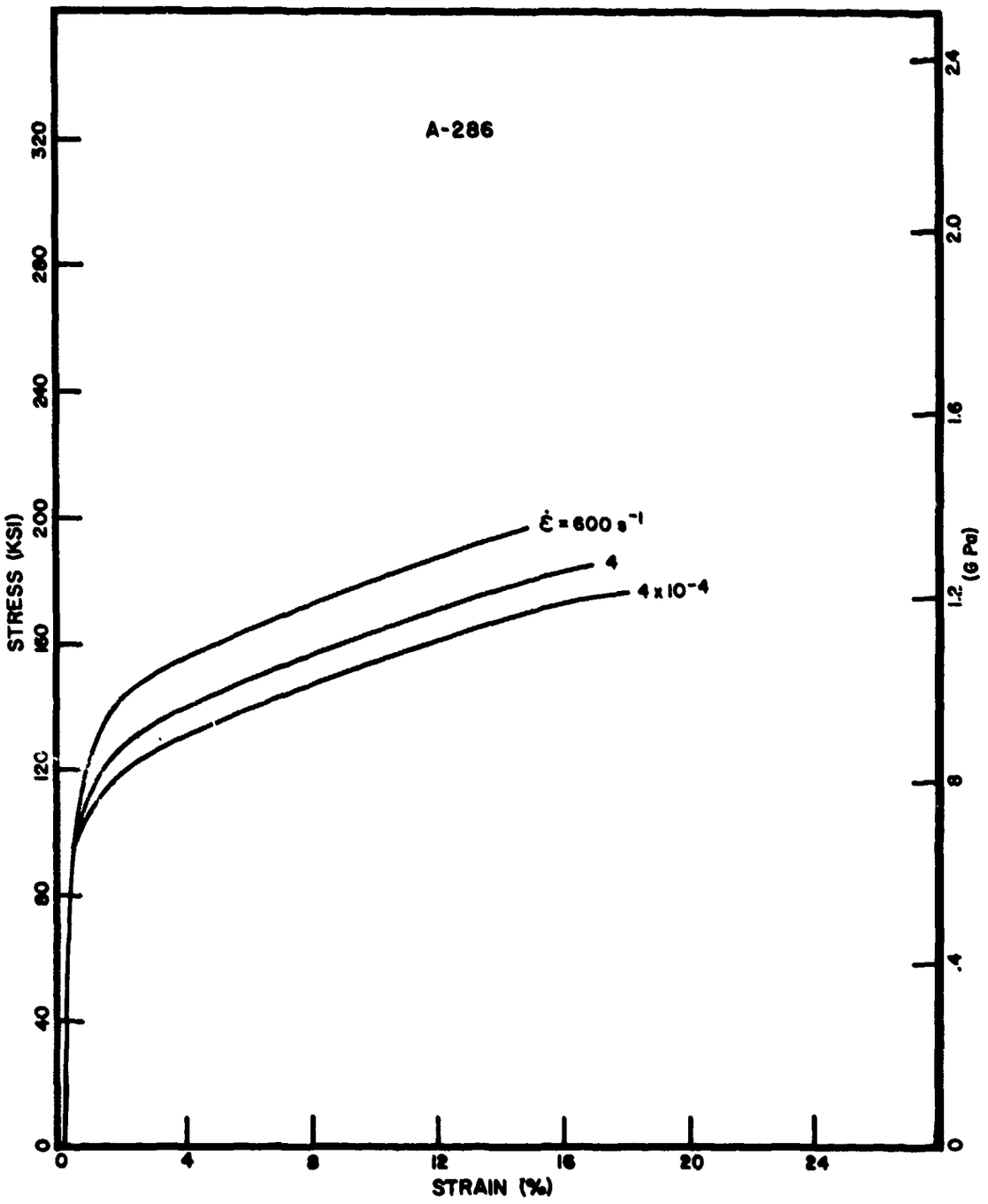

Figure 17. Stress-Strain Curves, A-286 Steel

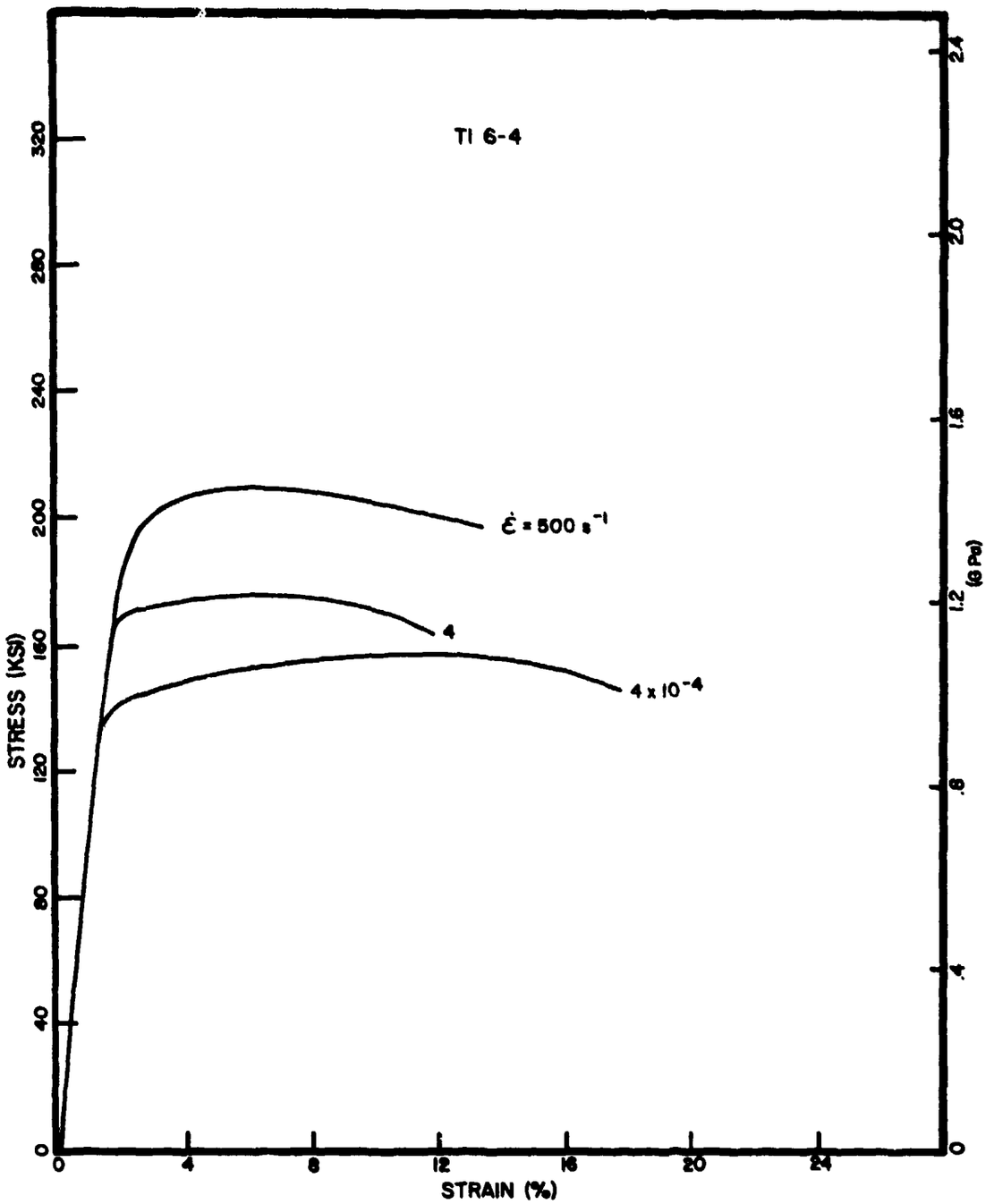

Figure 18. Stress-Strain Curves, Ti 6Al-4V

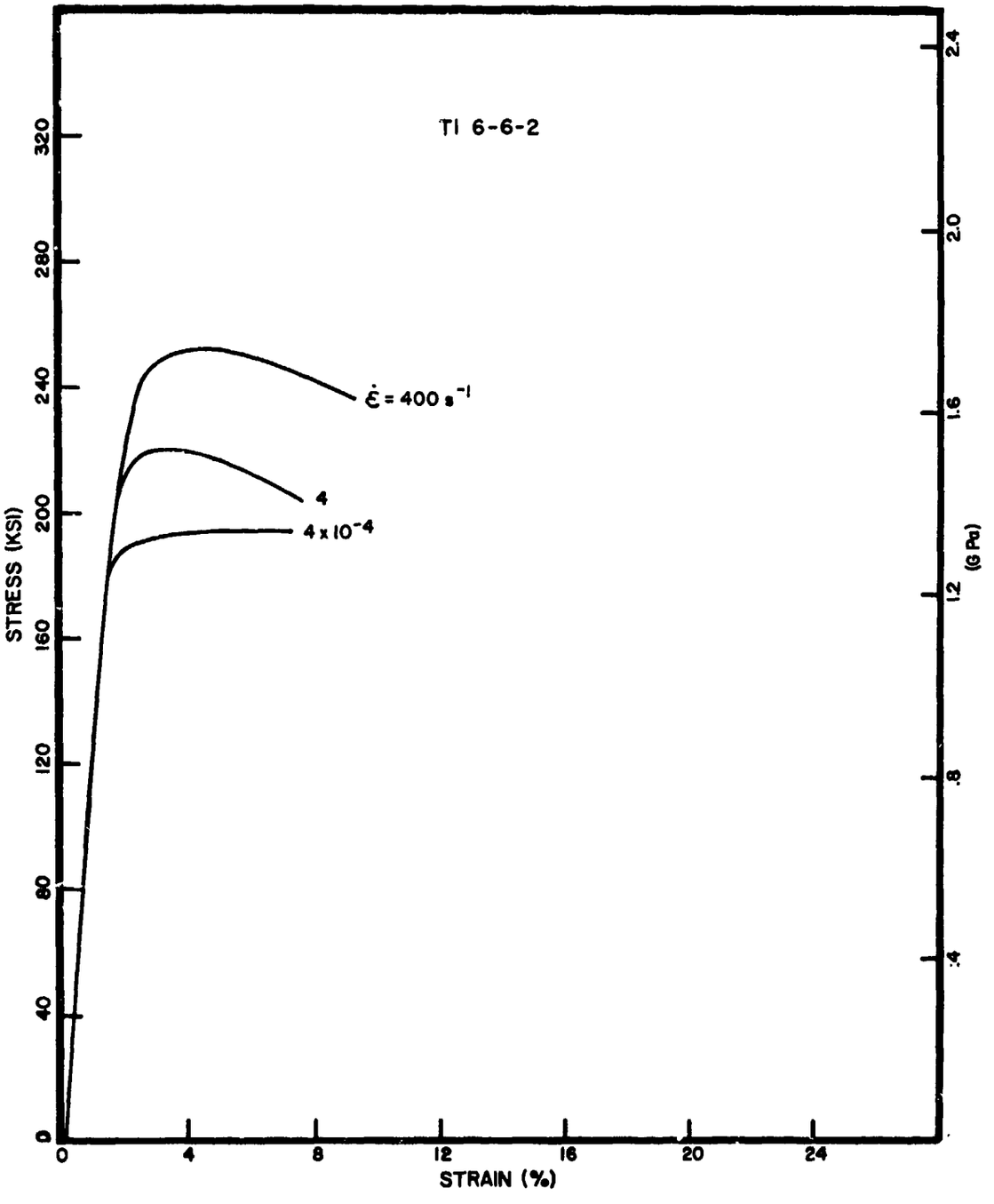

Figure 19. Stress-Strain Curves, Ti 6Al-6V-2Sn

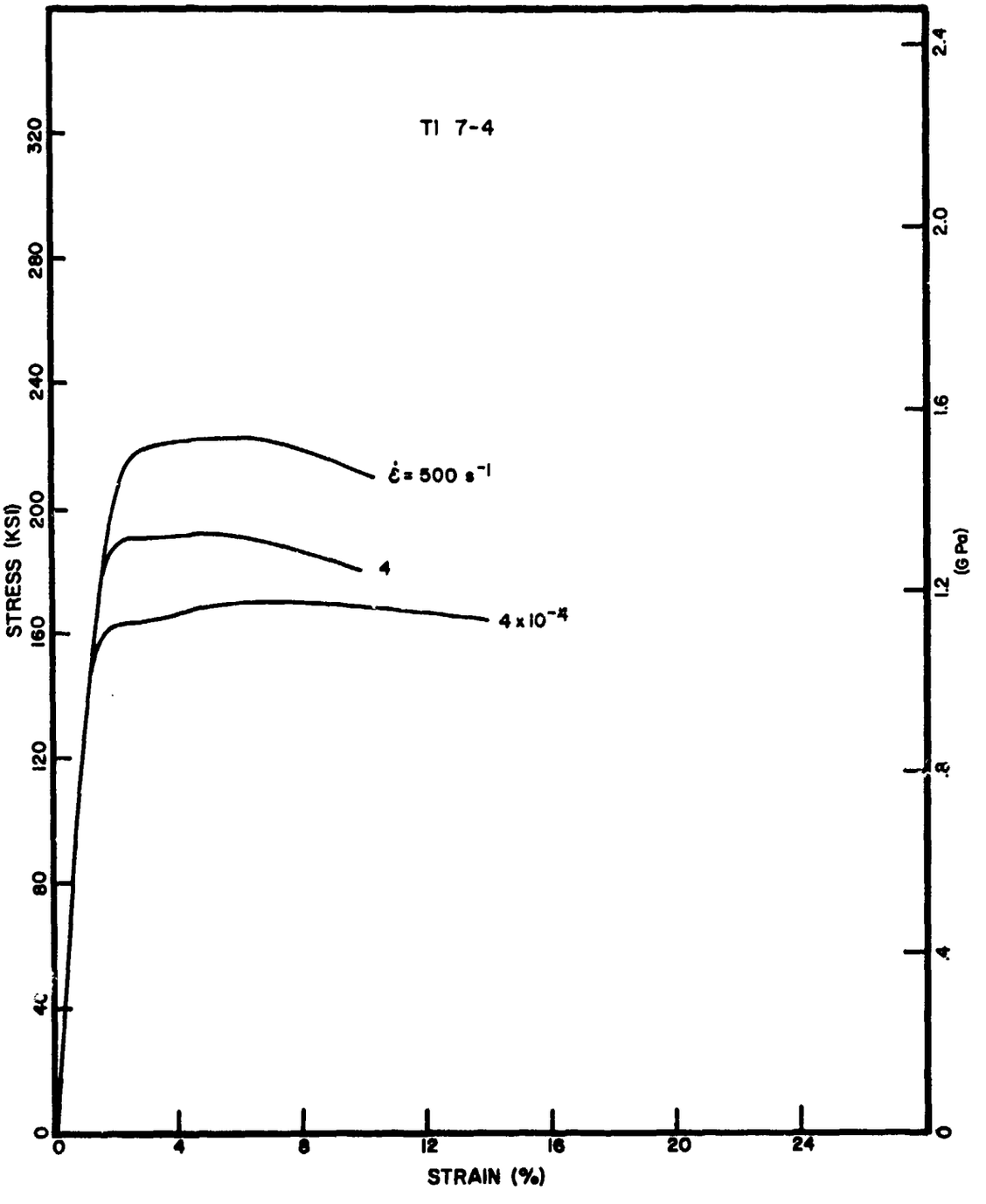

Figure 20. Stress-Strain Curves, Ti 7Al-4Mo

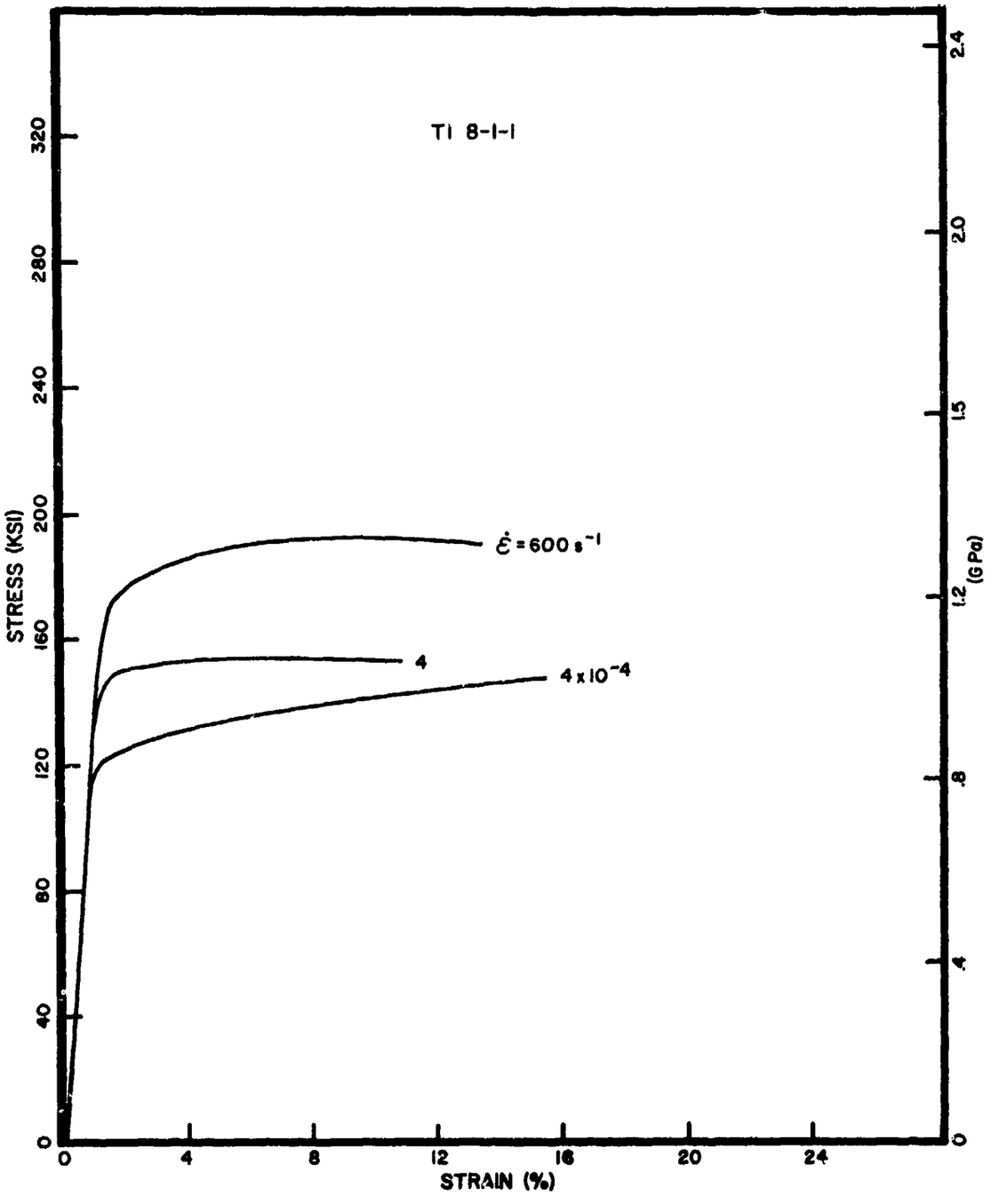

Figure 21. Stress-Strain Curves, Ti 8Al-1Mo-1V

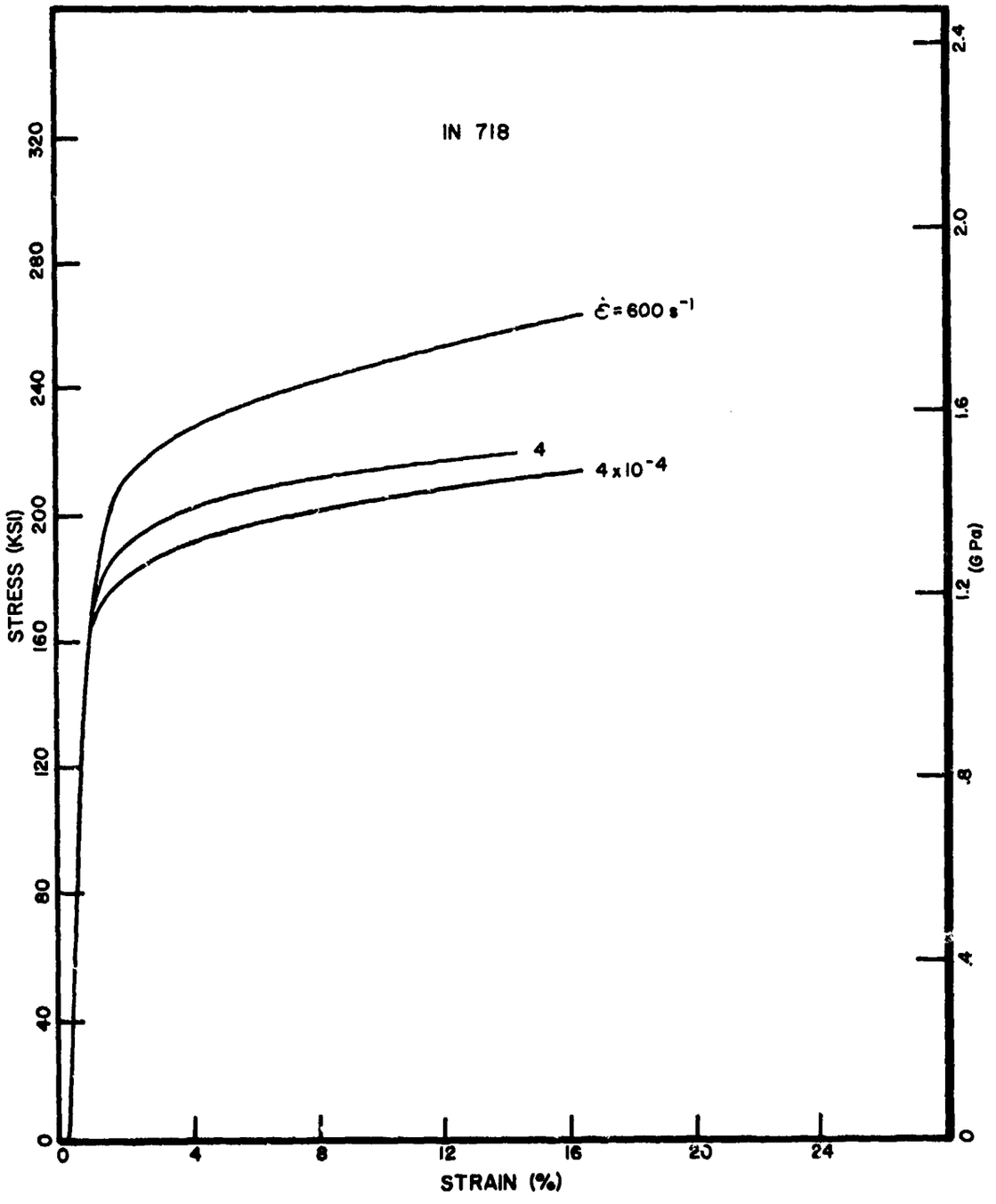

Figure 22. Stress-Strain Curves, IN718 Alloy

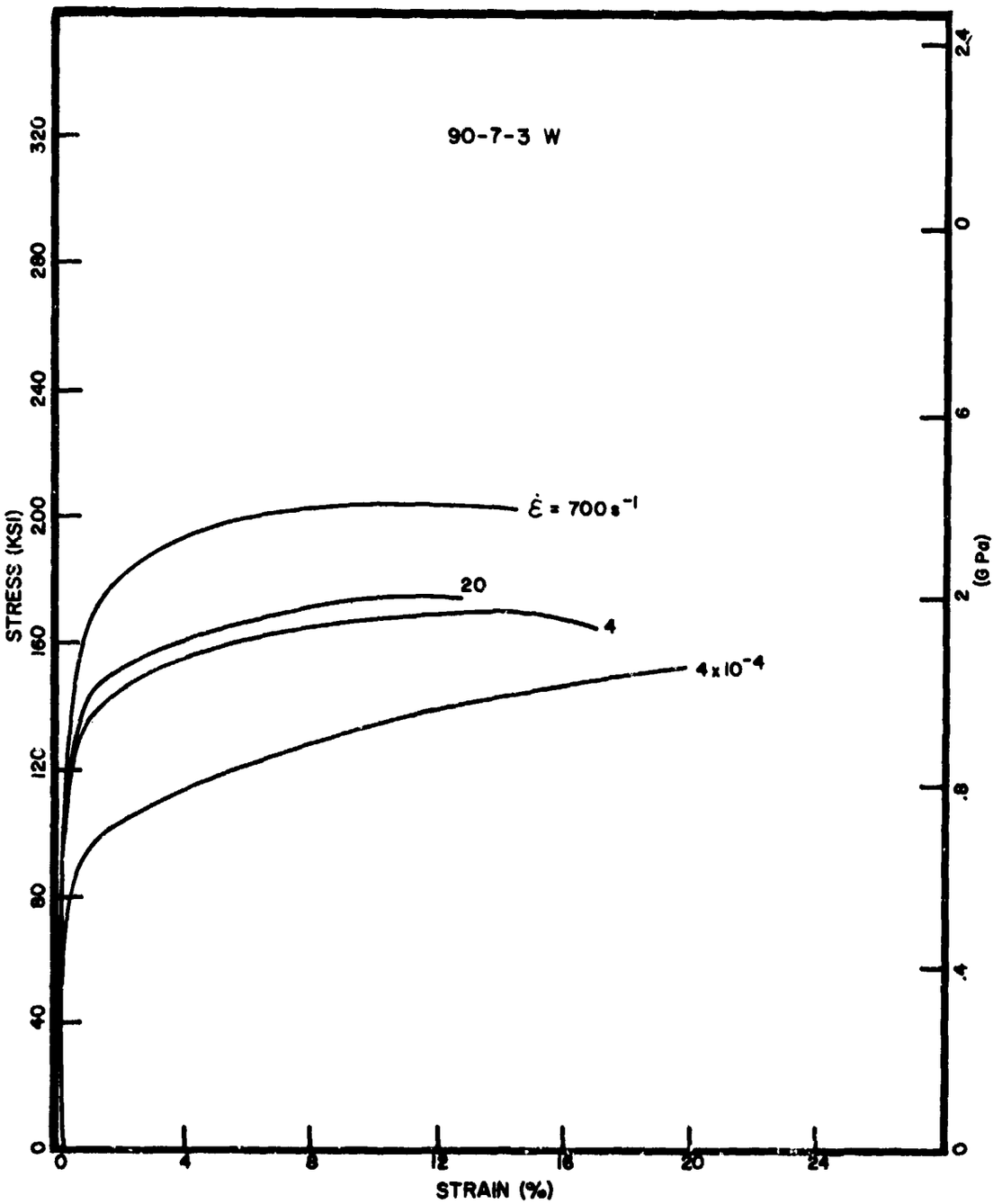

Figure 23. Stress-Strain Curves, Tungsten Alloy 90W-7Ni-3Fe

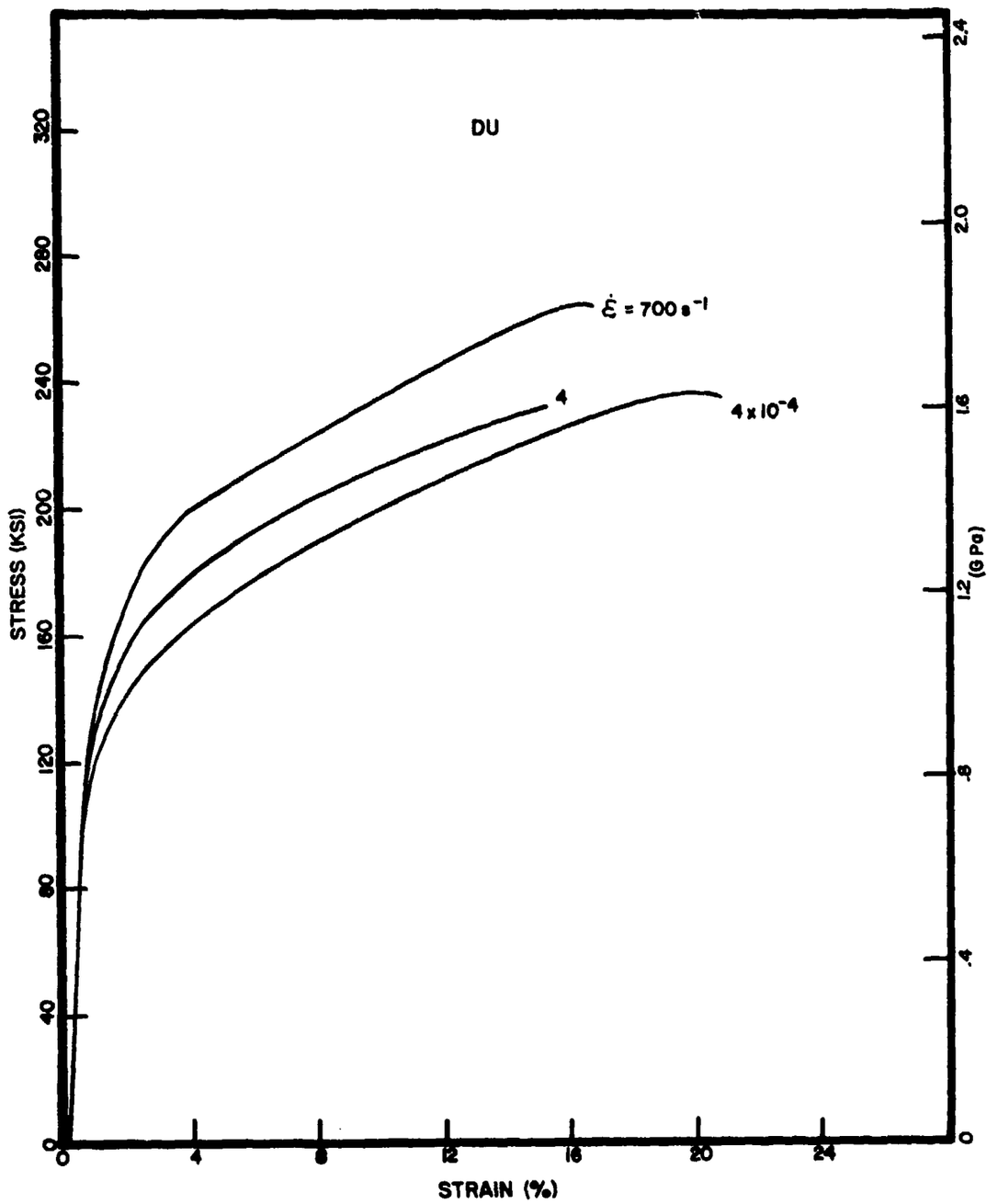

Figure 24. Stress-Strain Curves, Depleted Uranium

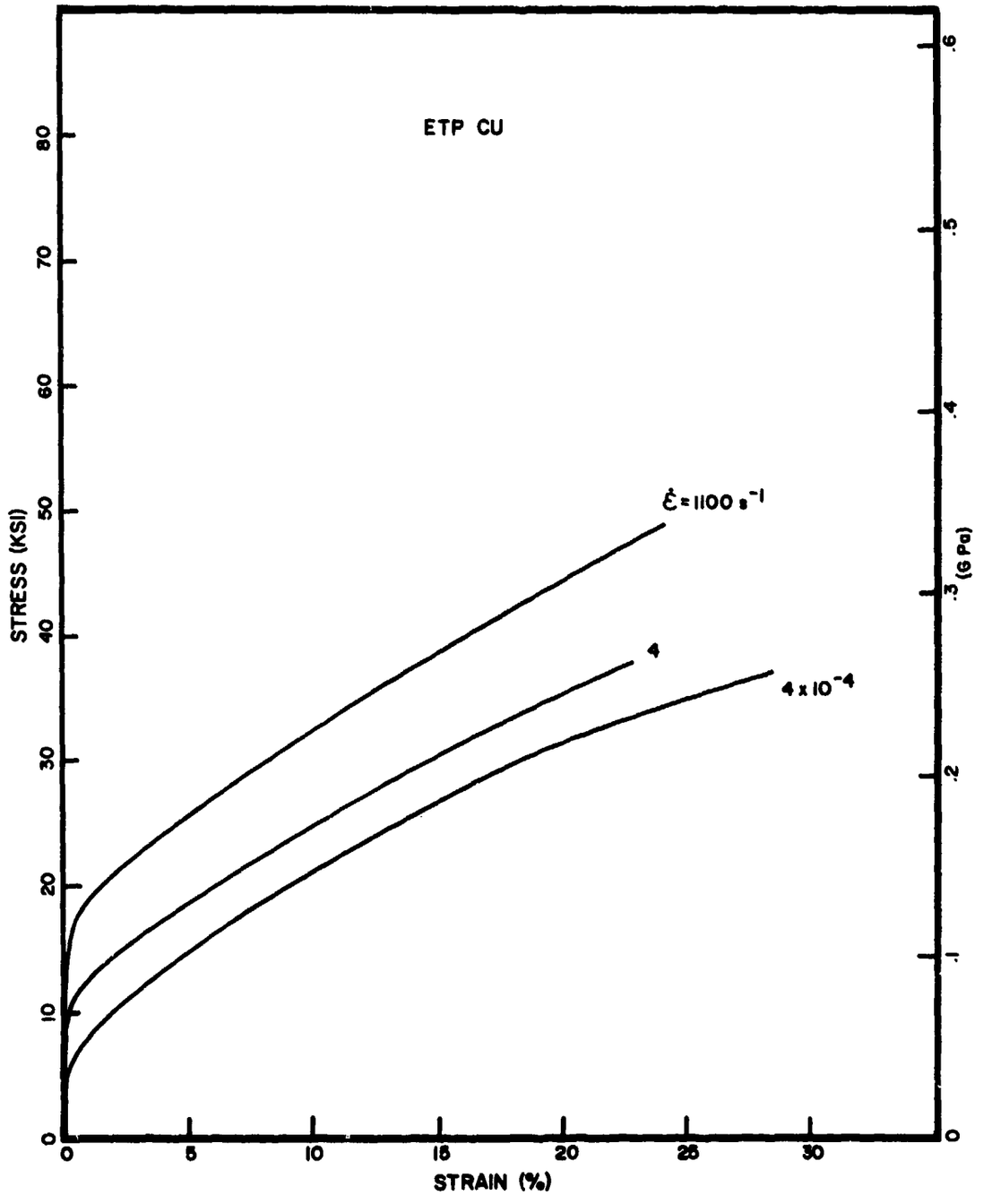

Figure 25. Stress-Strain Curves, ETP Copper

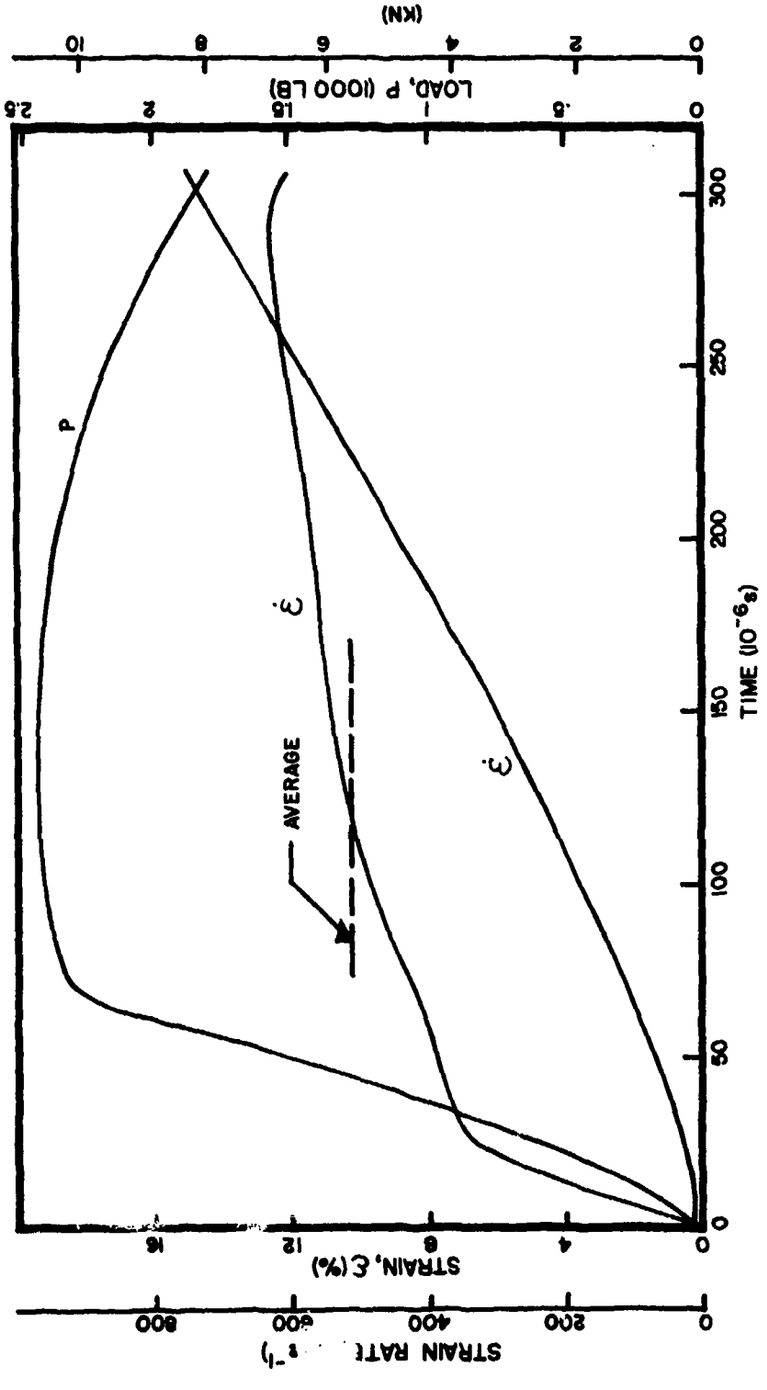

Figure 26. Typical Experimental Data, Ti6-4, Spec. No. 6L

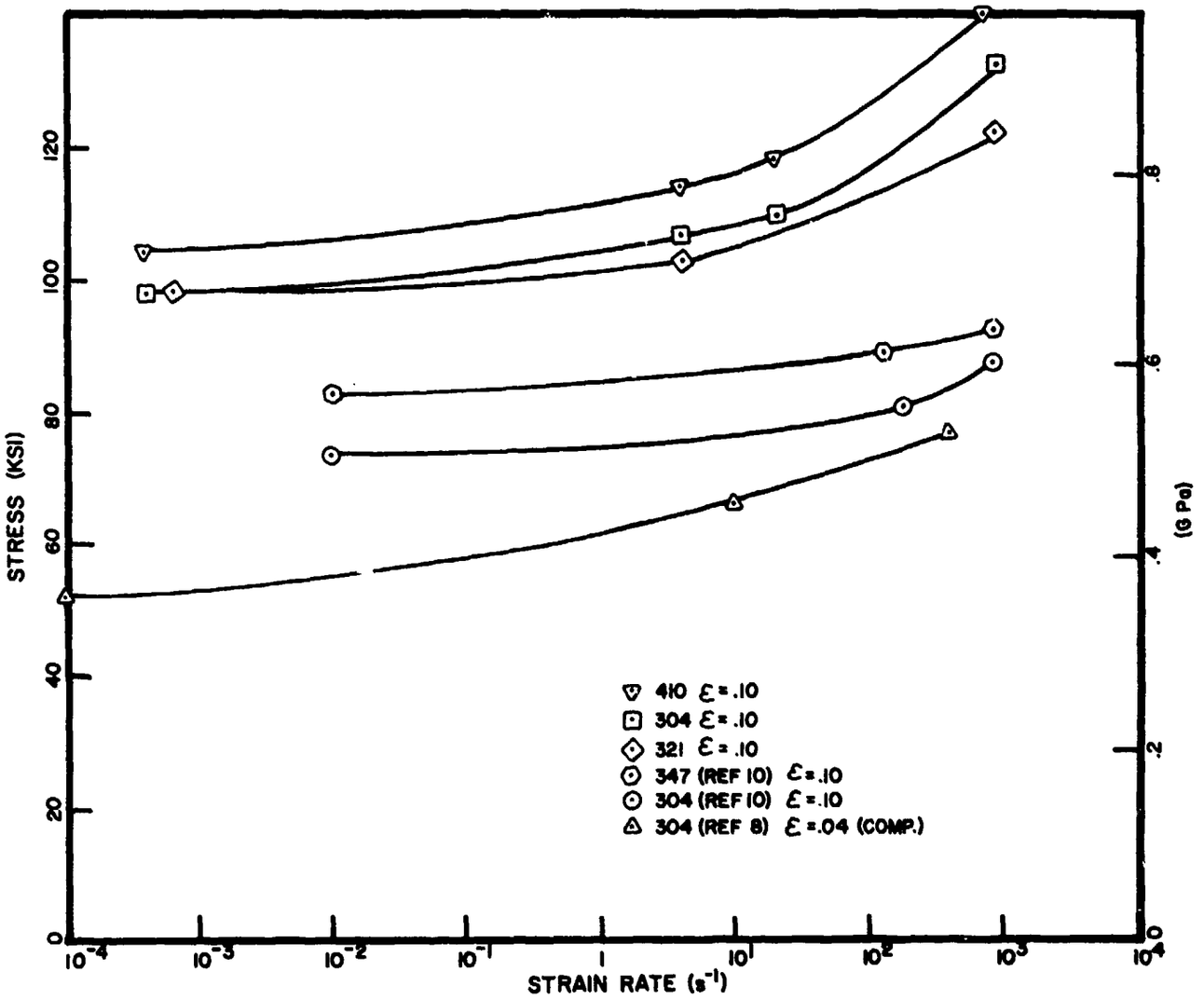

Figure 27. Stress-Log Strain Rate Data for Several Stainless Steels

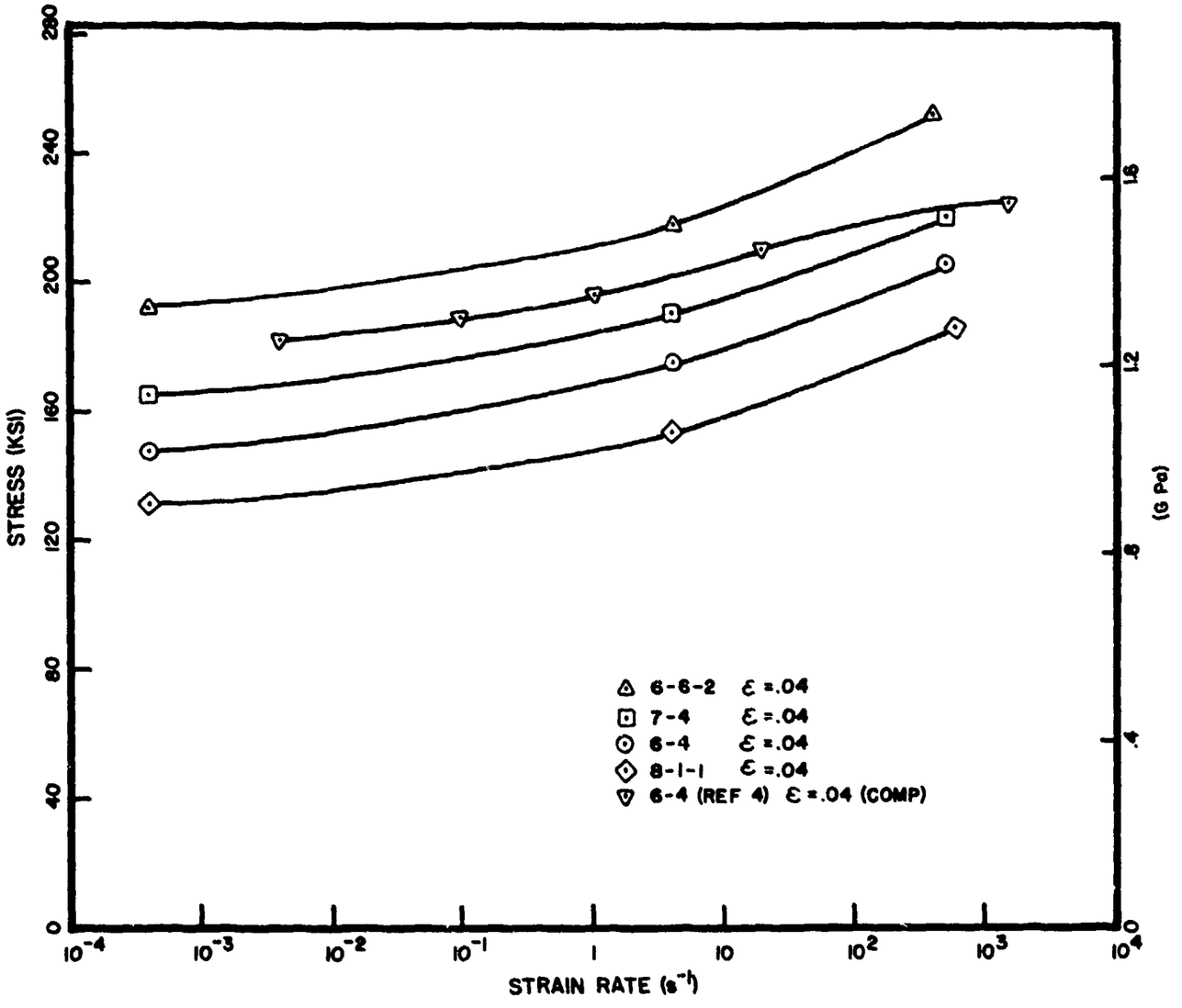

Figure 28. Stress-Log Strain Rate Data for Several Titanium Alloys

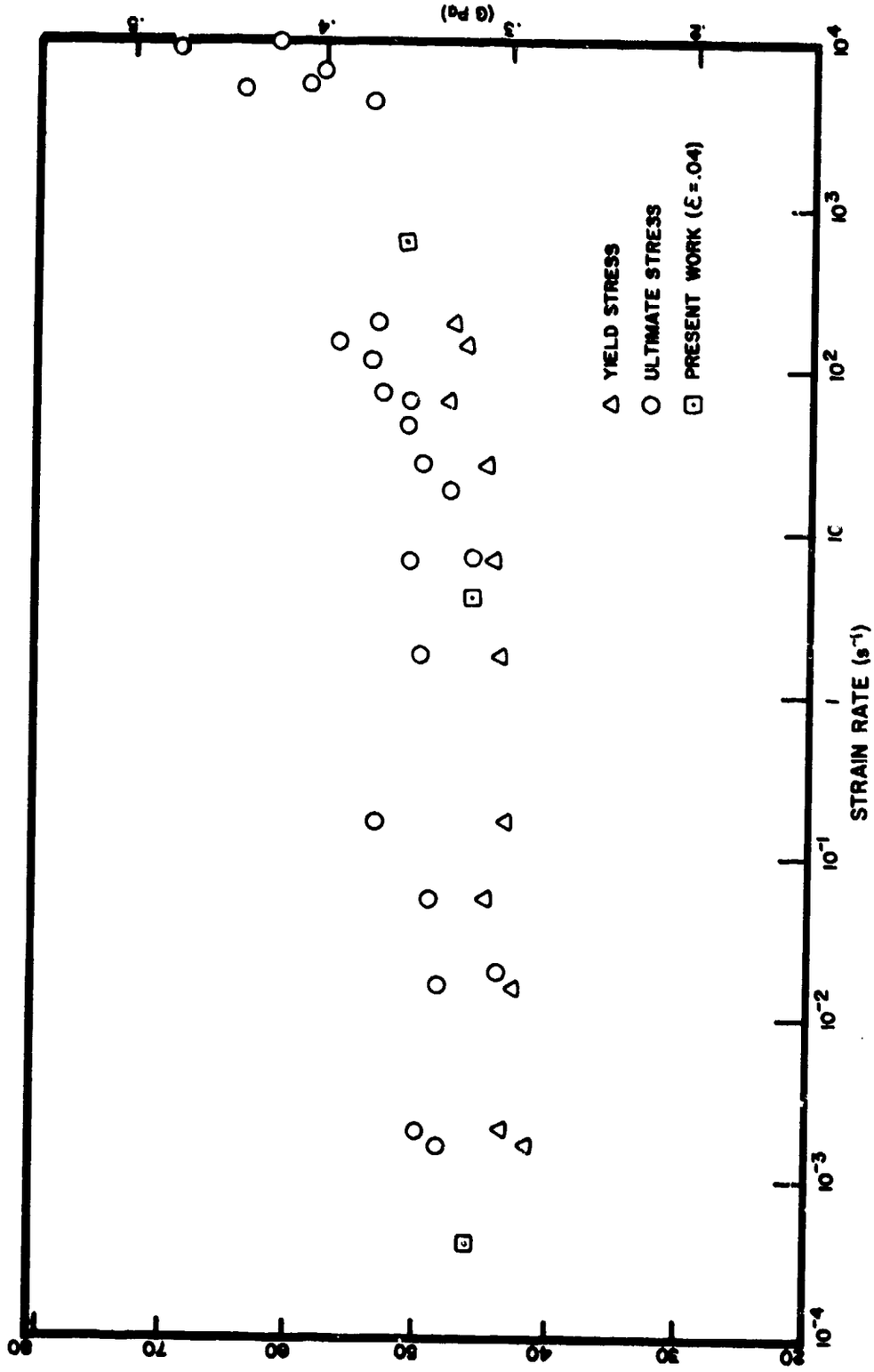

Figure 29. Yield and Ultimate Stress for Al 6061T-6 (From Fig. 1, Ref. 14)

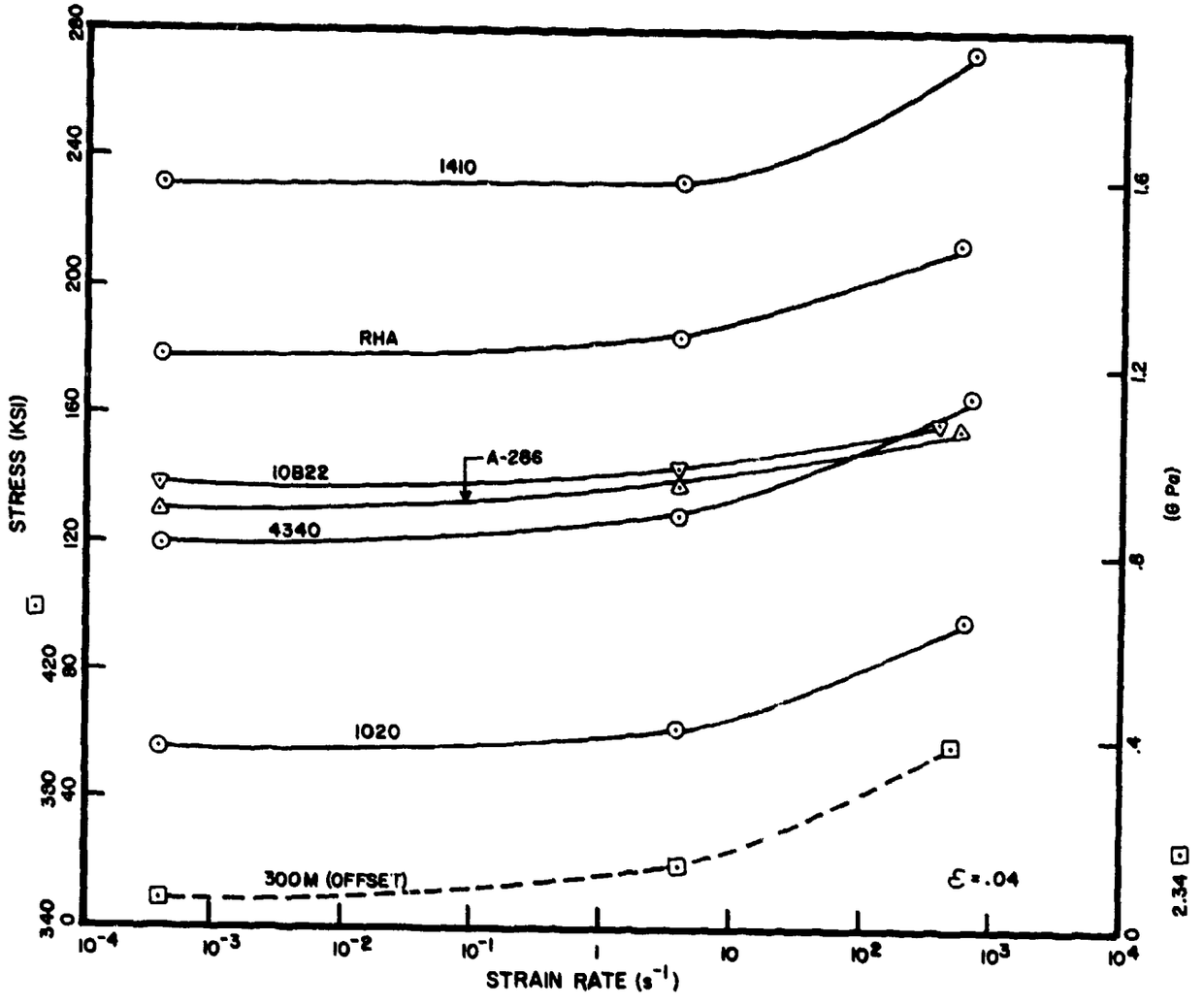

Figure 30. Stress-Log Strain Rate Data for Several Steels

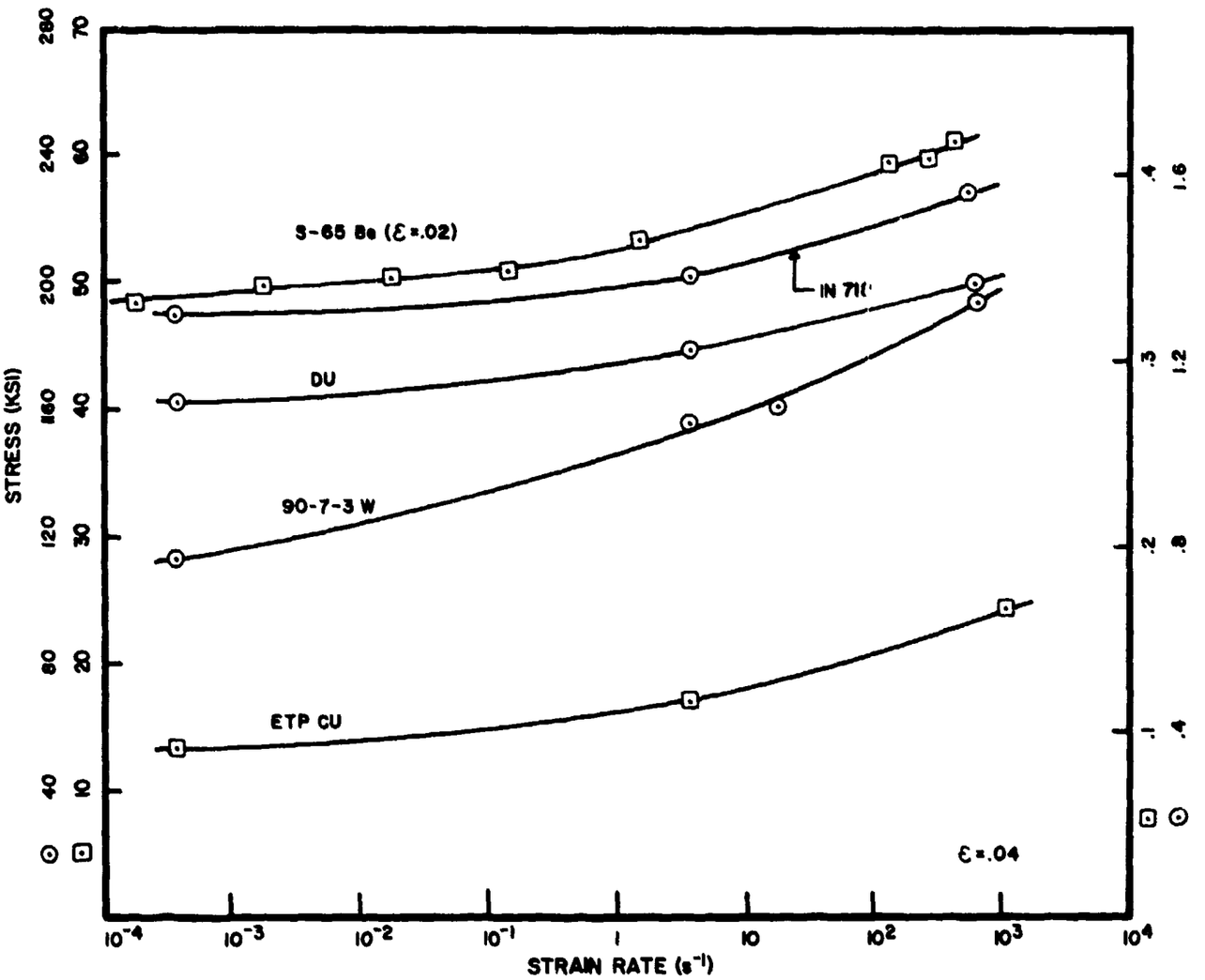

Figure 31. Stress-Log Strain Rate Data for Several Other Materials

REFERENCES

1. H. Kolsky, "An Investigation of the Mechanical Properties of Materials at Very High Rates of Loading", Proc Phys Soc (London), B62, 676-700 (1949).

2. U. S. Lindholm, "High Strain Rate Tests", in Techniques of Metals Research, Vol 5, Part 1, Ed. by R. F. Bunshah, John Wiley and Sons, 1971.

3. U. S. Lindholm, "Some Experiments with the Split Hopkinson Pressure Bar", J. Mech. Phys. Solids, 12, 317-335 (1964).

4. C. J. Maiden and S. J. Green, "Compressive Strain-Rate Tests on Six Selected Materials at Strain Rates From 10^{-3} to 10^{4} in/in/sec", J. Appl. Mech., 33, 496 (1966).

5. D. L. Holt, S. G. Babcock, S. J. Green and C. J. Maiden, "The Rate Dependence of the Flow Stress of Some Aluminum Alloys", Trans ASM,60 152 (1967).

6. U. S. Lindholm and L. M. Yeakley, "High Strain Rate Testing: Tension and Compression," Expt. Mech., 8, 1-9 (1968).

7. D. R. Christman, W. M. Isbell, S. G. Babcock, A. R. McMillan and S. J. Green, "Measurements of Dynamic Properties of Materials, Vol II, Experimental Methods and Techniques", Final Report under Contract DASA01-68-C-0114, Report No. DASA 2501-2, MSL 70-23, Vol II, August 1971.

8. F. E. Hauser, "Techniques for Measuring Stress-Strain Relations at High Strain Rates", Expt Mech, 6, 395 (1966).

9. J. Harding, E. O. Wood and J. D. Campbell, "Tensile Testing of Materials at Impact Rates of Strain", J. Mech Eng Sci, 2, 88-96 (1960).

10. C. Albertini and M. Montagnani, "Testing Techniques Based on the Split Hopkinson Bar", in Mechanical Properties at High Rates of Strain, The Institute of Physics, London, 1974.

11. T. Nicholas, "Mechanical Properties of Structural Grades of Beryllium at High Strain Rates", Report No. AFML-TR-75-168, Wright-Patterson AFB, OH, Oct 1975.

12. R. F. Steidel and C. E. Makerov, "The Tensile Properties of Some Engineering Materials at Moderate Rates of Strain", ASTM Bulletin 247, 57-64 (1960).

13. U. S. Lindholm and R. L. Bessey, "A Survey of Rate Dependent Strength Properties of Metals", AFML-TR-69-119, Wright-Patterson AFB, Ohio, April 1969.

REFERENCES (CONCLUDED)

14. C. W. Jiang and M. M. Chen, "Dynamic Properties of Materials, Part II - Aluminum Alloys", Report No. AMMRC CTR 74-23, Watertown, Mass. April 1974.

15. J. E. Smith, "Tension Tests of Metals at Strain Rates up to 200 sec^{-1}", Materials Research and Standards, 713-718 (1963).

16. U. S. Lindholm, R. L. Bessey, and G. V. Smith, "Effect of Strain Rate on Yield Strength, Tensile Strength, and Elongation of Three Aluminum Alloys", Jour. of Materials, JMLSA, 6, 1, 119-133 (1971).

17. K. G. Hoge, "Influence of Strain Rate on Mechanical Properties of 6061-T6 Aluminum Under Uniaxial and Biaxial States of Stress", Expt Mech. 6, 209-211 (1966).

18. A. L. Austin and R. F. Steidel, Jr., "The Tensile Properties of Some Engineering Materials at High Rates of Strain", Proc. ASTM, 1292-1308 (1959).

19. S. J. Green and S. G. Babcock, "High Strain Rate Properties of Eleven Reentry-Vehicle Materials at Elevated Temperatures", Part I of Final Report for DASA Contract DA-49-146-XZ-322, TR 66-83, Part I, Nov 1966.

☆U.S.Government Printing Office: 1980 — 757-002/226